

The Mediterranean Sea: Present and Past

Rohling, E.J., Abu-Zied, R., Casford, J.S.L., Hayes, A., and Hoogakker, B.A.A.

1. Introduction

The Mediterranean is a landlocked, semi-enclosed marginal sea which spans a maximum of 3860 km in the W-E direction, and a maximum of ~1600 km in the N-S direction. Along its roughly 46,000 km of coastline, the basin is enclosed by mountainous terrain, except for a part of the North African margin to the east of Tunisia. The Mediterranean Sea contains very deep basins that reach more than 4 km depth, and has an average depth of approximately 1500 m. Its only natural connection with the open (Atlantic) ocean is through the narrow Strait of Gibraltar, which contains a 284 m deep sill (at a width of ~30 km), and which reaches a minimum width of only 14 km (at a depth of 880 m) (Bryden and Kinder, 1991). The Strait of Sicily subdivides the Mediterranean Sea into a western and an eastern basin. This strait is relatively wide (about 130 km) and contains a topographically complex sill-structure with an estimated average depth of 330 m (Wüst, 1961), reaching 365 and 430 m in the two major channels (Garzoli and Maillard, 1979). The eastern Mediterranean contains two smaller marginal basins, namely the Adriatic Sea and the Aegean Sea ([Figure 1](#)).

Watermasses are exchanged through both the Strait of Gibraltar and the Strait of Sicily by eastward surface and westward subsurface flows ([Figure 2](#)). This pattern of exchange results from a net buoyancy loss in the basins on the easterly side of the sills, primarily due to strong net evaporative loss from the Mediterranean, and secondarily to some net cooling. Deepwater ventilation in the Mediterranean is primarily salt-driven, and secondarily temperature-driven. This is similar to the mode observed in the present-day Red Sea, but contrasts with the temperature-dominated mode in the modern world ocean. As such, the Mediterranean deep ventilation might be more appropriately described as halo-thermal rather than with the common term thermo-haline. This offers a useful analogue for world ocean circulation modes in past times with very warm and relatively equable global climates, such as the Mesozoic. Interestingly, the Mediterranean is characterised by periodic, widespread deposition of organic-rich sediments or “sapropels” over periods of several thousands of years, similar (in miniature) to the deposition of “black shales” in the Mesozoic oceans.

Surface water flowing in through the Strait of Gibraltar is traceable through the Strait of Sicily into the eastern Mediterranean, although its salinity increases steadily towards the east (e.g., Wüst, 1961; Malanotte-Rizzoli and Hecht, 1988; Malanotte-Rizzoli and Bergamasco, 1989; Pinardi and Masetti, 2000) ([Figures 2,3](#)). The eastward salinity increase culminates in values around 39.2 p.s.u. (up to an extreme of 39.5 p.s.u., Wüst, 1960) in the eastern Levantine sector of the Mediterranean, compared with 36.1-36.2 p.s.u. for the Atlantic inflow at Gibraltar. The high Levantine salinities are associated with high temperatures in summer, but strong winter cooling (especially between Cyprus and Rhodes) causes surface waters to attain high enough densities to sink and spread at intermediate depths (150-600 m). This forms the “Levantine Intermediate Water (LIW)”. This watermass spreads westward from its formation area throughout the entire Mediterranean Sea.

Admixtures of regional winter mixed-layer waters slightly reduce the LIW salinity as it spreads, transforming this watermass into what has become known as “Mediterranean Intermediate Water (MIW)”. There are also contributions of Eastern Mediterranean Deep Water (EMDW) and Western Mediterranean Deep Water (WMDW) to the MIW upon its passage through the Strait of Sicily and the Strait of Gibraltar. In most parts of the eastern Mediterranean, MIW salinities are between 38.8 and 39.1 p.s.u., while values in the western Mediterranean are between 38.5 and 38.8 p.s.u. The subsurface outflow from the Mediterranean through the Strait of Gibraltar has a salinity of 38.2-38.4 p.s.u. (among many others: Wüst, 1960, 1961; Garzoli and Maillard, 1979; Gascard and Richez, 1985; Bryden et al., 1994).

The influence of Mediterranean Outflow can be traced as a salinity maximum centred on about 1000 metres depth in the North Atlantic (e.g., Reid, 1979; Hill and Mitchelson-Jacob, 1993; Iorga and Lorzier, 1999, O'Neill-Baringer and Price, 1999). This maximum represents the overall average signature, but an important component of the dispersal of Mediterranean Outflow within the North Atlantic has been found to occur in the form of discrete subsurface “lenses” of salty and warm Mediterranean water. These are the so-called Mediterranean eddies or “Meddies” with diameters up to 100 km, the pathways of which have been traced with neutral-buoyancy floats (Richardson et al., 1991, 2000). The isopycnals at which Mediterranean outflow settles show northward shoaling within the NE Atlantic. Near the Iceland-Scotland Ridge deep winter mixing of fresher surface waters with the salty Mediterranean tongue raises the salinity of the surface water that enters the Norwegian Sea through the Faroe-Shetland Channel (Hill and Mitchelson-Jacob, 1993). This preconditions the inflow for later convection by increasing its salinity by several tenths of a p.s.u. relative to ‘background’ (Reid, 1979), the density equivalent of 1-2° C cooling. Such preconditioning may facilitate the formation of North Atlantic Deep Water (NADW) in the Norwegian Sea (Reid, 1979; Hill and Mitchelson-Jacob, 1993).

Returning attention to the Mediterranean now, EMDW and WMDW are found below about 1 km depth in the eastern and western Mediterranean basins, respectively, separated by the sill in the Strait of Sicily. Between about 600 and about 1000 m, a transitional watermass is found between the deep waters and MIW. WMDW is formed in the northern sector of the western Mediterranean, notably in the Gulf of Lions, due to strong winter cooling caused by cold continental air outbreaks that are orographically channelled towards the basin via the Rhone valley (the “Mistral”). EMDW is formed in two separate regions, namely the Adriatic Sea and the Aegean Sea. Both areas are subject to orographically channelled continental air outbursts in winter, the “Bora” over the Adriatic, and the “Vardar” over the Aegean Sea (see [Chapter 4](#)).

In schematic terms, the Mediterranean deepwater ventilation can be viewed as a two-stage motor (a detailed explanation follows in section 3). The first stage consists of the dominantly salt-driven formation of LIW. The salt distributed throughout the Mediterranean Sea by LIW/MIW preconditions the basin for deepwater formation. The second stage of the deep-ventilation motor is dominated by cooling events related to orographically channelled continental air outbursts over northern sectors of the basin in winter. Given the presence of a major monsoon-fed river (Nile) in close proximity to the centre of action of the salt-driven first stage of the motor, we can expect that monsoon variations would be reflected in the efficiency of the

Mediterranean's deep ventilation, as deepwater preconditioning would be directly affected. However, we can also expect important northerly climate impacts on the deep ventilation, related to changes in the frequency and/or intensity of winter cooling events.

The small volume of the Mediterranean Sea, compared with ocean basins, causes changes in its climatic forcing to be recorded virtually instantaneously in palaeoceanographic proxy data, such as stable isotope and other geochemical ratios, and microfossil abundances. The basin's limited communication with the open ocean implies that any climatic signals will be recorded in an amplified fashion in Mediterranean properties, such as salinity and specific elemental concentrations. The critical location of the Mediterranean Sea on the boundary between a subtropical/monsoon regime and the temperate westerlies means that it is highly sensitive to changes in both these systems. Since both systems primarily affect fundamentally different characteristics of the basin, the Mediterranean is an excellent site for study of the relative timing and impact of changes in the two major systems (subtropical/monsoon climate predominantly affects freshwater balance, while the temperate westerly climate controls cooling in the north). The regularly recurring deposition of organic-rich "anoxic" sapropels offers discrete windows for very high-resolution study, since these intervals are not affected by sediment homogenisation due to bioturbation. The Mediterranean Sea may hold important clues as to the functioning of circulation in the Mesozoic oceans and the formation processes of black shales that are of great economic importance.

To fully appreciate the processes underlying past changes in Mediterranean climate and hydrography, comprehensive background knowledge of present-day conditions is indispensable. Following a brief history of the development of the Mediterranean basin, therefore, this chapter first discusses relevant aspects of the region's modern climate and oceanography, before engaging into a review of palaeoclimatological and palaeoceanographic reconstructions.

2. Long-term context

Chapter 2 of this book deals with the long-term tectonic history of the Mediterranean basin, and this section therefore only highlights several particularly relevant aspects of change in the climatic and oceanographic setting.

Overall, the Mediterranean is a relic ocean basin, representing the final stage of closure of the Tethys Ocean prior to continent-continent collision as the African plate converges with the Eurasian plate system. Note, however, that parts of the western basin are relatively young, and actively opening and deepening – notably the Tyrrhenian Sea. The proto-Mediterranean's eastern connection with the open ocean (through the Levantine-Arabian region) closed roughly 18 million years ago (Ma) (Vergnaud-Grazzini, 1985). Since that time, the only connection of the Mediterranean basin with the open world ocean has been through waterways in the west. Two such waterways connected the Mediterranean with the Atlantic Ocean: one across N Morocco (Rifian Strait) and one through the southern Iberian Peninsula (Betic Strait). Tectonic closure of the Betic and Rifian Straits led to massive evaporite deposition between 5.9 and 5.5 Ma, a phase known as the "Messinian salinity crisis" (followed by the so-called "Lago Mare" phase 5.5-5.3 Ma) (Hilgen et al., 1995).

Re-establishment of open marine conditions following the Messinian salinity crisis appears to have been virtually synchronous everywhere in the Mediterranean basin, and may be ascribed to the tectonic opening of the Strait of Gibraltar. This event heralded the appearance of a basin that clearly began to approach the modern configuration. However, ongoing plate subduction processes (including slab detachment underneath southern Italy) caused continuing highly complex tectonic re-shaping in the area. For example, the Tyrrhenian Sea underwent very rapid deepening and extension between ~3 and ~1.5 Ma, while tremendous uplift in southern Italy and parts of Greece has caused late Pliocene/early Pleistocene coastal sediments to be displaced to many hundreds of metres above modern sea level.

The basin's geological history can directly affect modern processes. When faults expose parts of the massive Messinian evaporite deposits to seawater in the basin, salt dissolution affects modern bottom-water properties. This happens in the so-called "brine basins" of the eastern Mediterranean. Dissolved salts in the bottom waters of these isolated depressions cause extremely high salinities, separated from the normal deep waters by a very sharp salinity gradient (halocline), which defines a strong density gradient (pycnocline). The oceanography and chemistry of brine basins are entirely different than in the open waters around them. Because of the extreme density stratification, the brines are not ventilated, and thus have become entirely oxygen-depleted. Sediments in these basins are often disturbed by mass-transport processes, but on rare occasions undisturbed sections yield beautifully laminated cores, reflecting the fact that there is no benthic life to homogenise the sediments through bioturbation (among many others: Jongsma et al., 1983; Scientific Staff Cruise BAN84, 1985; Troelstra et al., 1987; MEDRIFF consortium, 1995; Wallmann et al., 1997).

Major "global" climate developments also need to be considered when studying palaeoclimatic and palaeoceanographic signals in the Mediterranean. The development towards a "glacial mode" in the northern hemisphere started around 3.2 - 3.1 Ma (Shackleton and Opdyke, 1977; Thunell and Williams, 1983; Prell, 1984). The Mediterranean environment was substantially affected by the northern hemisphere glaciations (Vergnaud-Grazzini, 1985; Thunell et al., 1987, 1991). Ruddiman et al. (1987) found the first clear evidence for ice-rafting in the North Atlantic around 2.55 Ma, and Zachariasse and Spaak (1983) demonstrated that biogeographic patterns similar to the present originated around that time in the Mediterranean and adjacent Atlantic. The early development of northern hemisphere glaciation was associated with climatic change over the Mediterranean basin, characterised by increasing seasonal contrasts with very dry summers (Suc, 1984; see also Thunell, 1986). Suc (1984) argued that the 'modern' conditions with cool wet winters and hot dry summers first developed around 3.2 Ma, and that summer drought became more persistent after 2.8 Ma. Global atmospheric circulation modelling by Ruddiman and Kutzbach (1989) suggests that these developments may have resulted from northern hemispheric climate reorganisation due to uplift of the Tibetan plateau, while the periodical appearance of steppe vegetation in the Mediterranean realm since 2.3 Ma (Suc, 1984) would be related to large-scale expansions of northern hemisphere ice-sheets. The early glacial cycles had a mean periodicity of 41,000 years (obliquity forcing), which changed to a predominant periodicity of 100,000 years (eccentricity forcing) after the so-called Mid-Pleistocene Transition, roughly 1.0 to 0.9 Ma (Shackleton and Opdyke,

1973, 1976; Pisias and Moore, 1981; Ruddiman et al., 1986, 1989). This change is well represented in Mediterranean isotopic, floral and faunal records (e.g. Zachariasse et al., 1989, 1990; Lourens et al., 1992; Vergnaud-Grazzini et al., 1993; [Chapter 5](#)).

3. Modern climate and oceanography

3.1. Climate

The classical Mediterranean climate is characterised by warm and dry summers, and mild and wet winters. As such, it appears opposite to monsoon climates, which instead comprise a pluvial maximum in the warm months. The Mediterranean climate regime is due to the basin's location on the transition between the climate conditions of the temperate westerlies that dominate over central and northern parts of Europe, and the subtropical high pressure belt over North Africa ([Figure 4](#)) (Boucher, 1975; Lolis et al., 2002; [Chapter 4](#)). In summer, the subtropical high pressure conditions are displaced to the north and most of the Mediterranean experiences drought, especially the south-eastern sector. Polar front depressions may still reach the western Mediterranean, but they only exceptionally penetrate the eastern Mediterranean (Rohling and Hilgen, 1991). During winter, the subtropical conditions are displaced southward, and the (northern sector of) the Mediterranean comes under the influence of the temperate westerlies with the associated Atlantic depressions that track eastward over Europe.

Polar and continental air masses over Europe are channelled towards the Mediterranean through valleys between the mountainous topography of the northern Mediterranean margin. During winter and spring, intense cold and dry katabatic air flows are channelled through the lower Rhone Valley towards the Gulf of Lions ("Mistral"), and also over the Adriatic and Aegean Seas ("Bora" and "Vardar"), causing strong evaporation and cooling of the sea surface (e.g., Leaman and Schott, 1991; Saaroni et al., 1996; Poulos et al., 1997; Maheras et al., 1999; Casford et al., 2003; and references therein). Conditions for northerly air flow into the western and eastern Mediterranean are determined by interaction between an intense low over the central or eastern Mediterranean, and NE-ward extension of the Azores High (over Iberia, France, and southern Britain) or westward ridging of the Siberian High towards NW Europe and southern Scandinavia (Maheras et al., 1999; Lolis et al., 2002). The winter-time low surface pressure conditions over the Mediterranean are a direct consequence of the high sea-surface temperatures due to the high thermal capacity of the basin's watermasses (Lolis et al., 2002). The most pronounced basin-wide cold winter events (complementing widespread cold conditions over Europe) develop in association with positive sea-level pressure anomalies to the west or northwest of the British Isles and particularly low pressure over the Mediterranean, a configuration that reflects an extreme phase of the North Atlantic Oscillation (NAO) (Moses et al., 1987; Maheras et al., 1999).

The main mode of climate variability in the Mediterranean is expressed by the so-called Mediterranean Oscillation (MO), a west-east pressure seesaw that is apparent both at the surface and at 500 hPa, especially in winter and spring (Maheras et al., 1999; Lolis et al., 2002). Statistical correlation has been found between the MO and the pressure seesaw of the NAO, where the low NAO index phase is associated with wet conditions in the western Mediterranean (Maheras et al., 1999; Lolis et al., 2002;

Dünkeloh and Jacobbeit, 2003; and references therein). This confirms previous observations of direct NAO impacts on the western Mediterranean, but for the eastern basin the relationship remains weakly established, except via dependence of the MO on the NAO (Dünkeloh and Jacobbeit, 2003). The statistically second main mode of winter variability, with important impacts on cyclogenesis in the basin and consequent precipitation in the northeastern and south-central parts of the Mediterranean, is the so-called Mediterranean Meridional Circulation (MMC) (Dünkeloh and Jacobbeit, 2003).

Cold and relatively dry northerly (meridional) air flow over warm sea surfaces causes intense cyclogenesis (formation of new depressions) in the northern sectors of the Mediterranean. Most cyclones observed in the Mediterranean are thus formed over the basin itself, although some Atlantic depressions may enter the (western) basin (Rumney, 1968; Trigo et al., 1999). Throughout the basin, however, winter cyclones are clearly linked to North Atlantic synoptic systems, as secondary lows when Atlantic systems interact with the Alps with additional cyclogenesis over the basin itself (Trigo et al., 2000). Cyclogenesis is most frequent in the western Mediterranean, especially over the Gulf of Genoa and Ligurian Sea, but the Aegean Sea is a major centre for winter-time cyclogenesis as well (Trewartha, 1966; Rumney, 1968; Boucher, 1975; Cantu, 1977; Trigo et al., 1999). The majority of Genoan depressions tracks south-eastward down the coast of Italy and then eastward or north-eastward across the Aegean Sea or northern Levantine seas (Trewartha, 1966; Rumney, 1968; Trigo et al., 1999; Lolis et al., 2002). Along the way, these depressions as well as those developing over other centres of cyclogenesis cause the winter precipitation that is so typical for the modern Mediterranean climate. The stable hydrogen and oxygen isotope composition of this precipitation follows a Mediterranean-specific mixing line (the Mediterranean Meteoric Water Line, MMWL), which is different from the global Meteoric Water Line (MWL) due to the dominant contribution of moisture evaporated from the Mediterranean Sea into low-humidity air masses (Matthews et al., 2000; and references therein).

Summer rainfall is low today, especially in the eastern basin. Although cyclogenesis occurs around Cyprus and the Middle East in summer, as a semi-permanent extension of the Indian monsoon low, dry summer conditions prevail as a consequence of adiabatic descent in the upper troposphere that is related to the intense Asian summer monsoon (Rodwell and Hoskins, 1996; Trigo et al., 1999).

Mean annual precipitation along the Mediterranean ranges from less than 0.12 m in North Africa, to over 2.00 m in portions of southwest Turkey and in the eastern Adriatic Sea along the slopes of the Dinaric Alps (Naval Oceanography Command, 1987). Total evaporation in the entire Mediterranean increases towards the east, with an average of 1.45 m y^{-1} (Malanotte-Rizzoli and Bergamasco, 1991) to 1.57 m y^{-1} (Bethoux and Gentili, 1994). Strong rates of evaporation occur in areas subjected to strong winds, such as the Gulf of Lions and Ligurian Sea, the Aegean and Cretan Seas and the southern part of the Turkish coast (MEDOC Group, 1970; Miller, 1974). Evaporation is weakest along the Moroccan and Algerian coasts (The Alboran Sea) where the air masses generally arrive from the Atlantic with relatively high air humidity.

The basin-wide mean Mediterranean excess of evaporation over freshwater input [E (evaporation) - P (precipitation) - R (runoff)] has been variously estimated at $\sim 1.00 \text{ m yr}^{-1}$ (Bethoux et al., 1999), 0.75 m yr^{-1} (Gilman and Garrett, 1994), and $0.56\text{--}0.66 \text{ m yr}^{-1}$ (Bryden and Kinder, 1991). There is marked spatial variation in regional values.

Northern areas such as the Gulf of Lions, Adriatic and Aegean Seas show relatively low excess evaporation rates due to high freshwater inputs from the Rhone and Ebro rivers, the Po river, and the Black Sea, respectively. Southern regions show very high excess evaporation rates, especially in the eastern Mediterranean (Béthoux and Gentili, 1994). The strong overall excess evaporation results in a pronounced surface water salinity increase from west to east (MEDATLAS, 1997) ([Figure 2](#)).

Sea surface temperature values in the Mediterranean reflect a balance dominated by high energy gain from solar irradiation during the widespread subtropical high-pressure (clear) conditions in summer, and considerable (latent) heat loss during evaporation. As a result, sea surface temperature values increase towards the east and south throughout the Mediterranean. Winter values are around 10° C in the north-western Mediterranean and 15° C in the south-eastern Mediterranean, while summer values are around 21° C in the north-western Mediterranean and 26° C in the south-eastern Mediterranean (Naval Oceanography Command, 1987). The warmest season centres on July-August and the coldest on February-March.

One further climate impact on the Mediterranean Sea must be mentioned. It concerns a “remote” influence by a climate system that does not itself penetrate into the basin, namely the African monsoon. It used to influence the Mediterranean mainly through Nile River discharge, but has been severely curtailed since completion of the Aswan High Dam in 1964. Prior to the anthropogenic control of the Nile, its average discharge was $8.4 \times 10^{10} \text{ m}^3 \text{ yr}^{-1}$ ($4.5 \times 10^{10} \text{ m}^3 \text{ yr}^{-1}$ in low-flood years to $15.0 \times 10^{10} \text{ m}^3 \text{ yr}^{-1}$ in high-flood years), which from the mid 1960s has dwindled to a negligible amount (Nof, 1979; Said, 1981; Wahbi and Bishara, 1981; Béthoux, 1984; Rohling and Bryden, 1992). Note that the reported discharge values illustrate that, even in the instrumental era, there was strong (3-fold) interannual variability between high and low discharge years, which was mainly related to variability in the monsoon-fed contribution of the Blue Nile and Atbara rivers (see below).

The Nile River comprises two different systems: the White Nile, which drains the equatorial uplands of Uganda in a regular, permanent manner; and the Blue Nile and Atbara, which drain highly seasonal African monsoon precipitation from the Ethiopian highlands. Nile hydrology has been summarised by Adamson et al. (1980) and Williams et al. (2000). In summary, these authors find that prior to extensive anthropogenic intervention (damming), a maximum of 30% of the annual discharge of the Nile originated from the White Nile, and a minimum of 70% from the Blue Nile/Atbara. The winter flow was dominated (83%) by the steady White Nile contribution, whereas the Blue Nile/Atbara component provides 90% of the flow in summer. This seasonal contrast results from a massive increase in the Blue Nile and Atbara discharge between a winter low and summer high (see also Table 1), with the monsoon-related peak occurring in the months August-October. The White Nile discharge shows a much smaller ratio of change between its annual peak and lowest monthly value (Table 1), and is highest between late September and January. Table 1 illustrates historical discharge values for the three main tributaries after Hurst (1944)

and Said (1981) (according to those observations, the White Nile contribution to total annual discharge amounts to only 14%).

Table 1. Contributions to total Nile discharge from the main tributaries (after Hurst, 1944; Said, 1981):

	Flood season (between August and October). Values in $10^6 \text{ m}^3 \text{ day}^{-1}$	Regular flowing of water (outside flood seasons). Values in $10^6 \text{ m}^3 \text{ day}^{-1}$
White Nile (from Lake Victoria=equatorial highlands)	70.0	37.5
Blue Nile (Ethiopia)	485.0	7.5
Atbara (Ethiopia)	157.0	0.0
Total	712.0	45.0

The total suspended sediment load transport to the Mediterranean coast before closure of the Nile by the Aswan High Dam exceeded $1.0 \times 10^8 \text{ tonnes yr}^{-1}$ (Sharaf El Din, 1977; El Dardir, 1994; Stanley, 1996). Since completion of the Aswan High Dam, there has been negligible Nile discharge and sediment transport into the Mediterranean through the Rosetta and Damietta outlets (UNDP/UNESCO, 1978). Instead, salt water entering the mouth of the Rosetta extends some 25 km up-stream to the Nile barrage at Mutubis. A little fresh water reaches the Mediterranean through the Manzalla, Burullus and Idku lagoon outlets, and by pumping of lake Maryut water to the sea at Alexanderia (Stanley and Wingerath, 1996). The suspended load that bypasses the Nile Delta to the shelf via Nile distributaries, lagoon outlets and canals is about 15% of the original (pre-dam) load (Stanley et al., 1998). Apart from damming, the freshwater flow and sediment flux into the Mediterranean Sea were also curtailed due to the extensive irrigation network of canals and drains covering the entire Nile delta.

Prior to its anthropogenic reduction, the Nile plume used to be distinctly traceable with the prevailing surface circulation in the easternmost Mediterranean, from the Nile delta east- and northward along the eastern Levantine coast. It caused a zone with notably reduced surface-water salinities and enhanced turbidity (suspended matter) (Reiss et al., 1999).

3.2. Surface-water circulation

Circulation in the Mediterranean Sea is driven by wind stress and thermohaline forcing (POEM Group, 1992). Atlantic water (AW) enters the Mediterranean Sea as a surface flow through the Strait of Gibraltar, compensating for the net evaporative loss from the basin and the subsurface outflow. AW enters with a salinity of about 36.2 p.s.u. and temperature of about 15° C (Bethoux and Gentili, 1994). As it migrates through the Strait of Gibraltar, AW mixes with upwelled Mediterranean Intermediate Water (MIW), creating Modified Atlantic Water (MAW) which has higher temperatures (16° C) and salinities (36.5‰) (La Violette, 1986; Tintoré et al., 1988; Arnone et al., 1990; Heburn and La Violette, 1990). In the Alboran Sea, MAW is present along the southern Spanish coast as a strong jet (speeds up to several kilometres an hour) approximately 20 km wide and extending to a depth of 150 m (Pistek et al., 1985). The strength of the jet initiates the formation of two anticyclonic gyres (Figure 5), the positions of which fluctuate on time scales of 3-4 weeks (Heburn and La Violette, 1990). As the MAW flows eastward along the Spanish coast to Almeria, it converges with resident Mediterranean waters. The subsequent deflection of MAW towards Oran on the Algerian coast forms a well defined frontal zone along the eastern edge of the Eastern Alboran Gyre (Figure 5). This front extends to a depth

of 200 m and has a width of approximately 35 km (Cheney and Doblar, 1982). The Almeria-Oran Front, as it is known, is thought to be a permanent feature, although its position and intensity are controlled by the degree of development of the Eastern Alboran Gyre (Tintoré et al., 1988).

To the East of the Alboran Sea, MAW is concentrated along the northern coast of Africa in the so-called Algerian Current. To its north, northward branches of the MAW form part of various larger-scale cyclonic gyres (Figure 3), while smaller anticyclonic gyres are found to the south of the Algerian Current. Waters flowing northwards on both sides of Corsica, the western and eastern Corsica currents, join and form the northern cyclonic gyres in the Gulf of Lions, where the Mistral winds in winter initiate a series of processes leading to the formation of Western Mediterranean Deep Water (WMDW) (e.g., MEDOC group, 1970; Gascard, 1978; Leaman and Schott, 1991; Robinson and Golnaraghi, 1994; Rohling et al., 1998; and references therein).

MAW enters the eastern Mediterranean through the Strait of Sicily with salinities between 37.0 and 38.5 p.s.u. (38.5 is the salinity at the flow reversal boundary; Garzoli and Maillard, 1979). It feeds the Ionian Current and Mid-Mediterranean Jet (MMJ) through the Ionian Sea and Levantine Basin, respectively. The MMJ bifurcates several times to form a series of cyclonic and anticyclonic gyres interconnected by jets flowing at speeds of 20-30 cm s⁻¹ (POEM-group, 1992) (Figures 3, 6). One branch of the Mid-Mediterranean Jet flows to Cyprus and then north- and westward to become the Asia Minor Current (Figure 3). It must be noted that salinity values of MAW increase steadily as it travels from west to east, due to continued evaporation (Wüst, 1961; Malanotte-Rizzoli and Hecht, 1988).

3.3. Intermediate-water circulation

During winter, surface waters in the Levantine Basin experience enhanced mixing and evaporation as a consequence of strong winds associated with cold, dry air masses tracking the eastern Mediterranean at this time of year (Ozsoy, 1981), especially in the Cyprus-Rhodes area. A subsequent combination of low temperatures (15-16°C) and high salinities (~39.2 p.s.u., with extremes to 39.5 p.s.u.; Wüst, 1960) in surface waters creates favourable conditions for vertical convection and the consequent formation of Levantine Intermediate Water (LIW). This watermass is characterised by a salinity maximum, and spreads throughout the eastern and western Mediterranean basins, forming the major constituent of the Mediterranean Intermediate Water (MIW) (Figure 2). It resides between 150 and 600 m water depth, and its transition to surface MAW is marked by a distinct salinity gradient, or halocline (Figures 2, 7). There is no comparable source region for intermediate water formation in the western Mediterranean basin.

From its source area, LIW/MIW flows westwards, penetrating the Ionian and Adriatic Seas. On approaching the Strait of Sicily, part of the subsurface watermass is re-circulated back within the eastern basin, while the remainder continues to enter the Western Mediterranean basin. The actual ratio of re-circulation to efflux remains to be established (POEM-group, 1992). At the Strait of Sicily, MIW remains distinctive within the water column, although with somewhat reduced temperature (14°C) and salinity (38.75‰) values compared to those in the LIW source area, due to later admixtures (Garzoli and Maillard, 1979). On leaving the Strait, MIW settles between

about 200 and 600 m, and splits into main branches going: into the Tyrrhenian basin; along the western side of Sardinia; and along the Algerian-Moroccan coastlines to exit through the Strait of Gibraltar from the Mediterranean into the North Atlantic. MIW enters the Alboran Sea at a depth between 200 and 600 m, with temperatures and salinities of 13.2°C and 38.5‰ respectively, flowing in a westward direction towards the Strait of Gibraltar at velocities of 1-2 cm s⁻¹ (Parrilla et al., 1986; Richez and Gascard, 1986).

Since the subsurface outflow through the Strait of Gibraltar displays temperature and salinity values of about 13°C and 38.2-38.4 p.s.u., compared to values of 15-16°C and 36.1-36.2 p.s.u. in the surface (AW) inflow (e.g., Wüst, 1960, 1961; Gascard and Richez, 1985; Bryden et al., 1994), it is obvious that the Mediterranean experiences both net evaporation and net cooling (Garrett, 1994). The subsurface Mediterranean Outflow has a flux in the order of 1 Sv (Bryden and Kinder, 1991) to 1.5 Sv (Bethoux and Gentili, 1994) (1 Sverdrup = 1 x 10⁶ m³ s⁻¹). It settles between 1000 and 1500 m depth in the North Atlantic Ocean (e.g., Wüst, 1960; Stommel et al., 1973; Reid, 1979; Price et al., 1993).

3.4. Deepwater circulation

The western and eastern Mediterranean basins each have their own source of deep water, which settles below the MIW. Western Mediterranean Deep Water (WMDW) is formed in the NW Mediterranean, particularly the Gulf of Lions, and Eastern Mediterranean Deep Water (EMDW) in the Adriatic and Aegean Seas. Today, there is such consistent deepwater ventilation from these regions that both the western and eastern Mediterranean are characterised by well-oxygenated deep and bottom waters, with oxygen concentrations typically varying in reported ranges of 4.0-4.7 ml l⁻¹ or 180-210 µmol kg⁻¹ (Wüst, 1960; McGill, 1961; Miller et al., 1970; Schlitzer et al., 1991; Klein et al., 1999; Roether and Well, 2001). The following two sections discuss the mechanisms for WMDW and EMDW formation in more detail.

3.4.1. Western Mediterranean Deep Water (WMDW)

The Gulf of Lions is the key area for the Western Mediterranean deep circulation. The surface circulation in this area is characterised by a distinct cyclonic gyre (MEDOC-group, 1970) ([Figure 6](#)). In winter (January/February), cold and relatively dry Mistral winds over this region initiate Western Mediterranean Deep Water (WMDW) formation. Three phases can be distinguished: (1) the preconditioning phase, (2) the violent mixing phase and (3) the sinking and spreading phase ([Figure 8](#)) (MEDOC-group, 1970).

During the preconditioning phase, a reduction occurs in the stability of the water column due to winter cooling that leaves surface waters with low temperatures (10-12°C), high salinities (38.40 p.s.u.), and consequently elevated densities (Wüst, 1961; MEDOC-group, 1970; Leaman and Schott, 1991). At this time mixing occurs in the surface waters but the vertical profile still remains a three-layered one: (1) a relatively fresh and cold surface layer, (2) a warm saline intermediate layer and (3) a cold and medium-saline deep layer ([Figure 8](#)). The onset of strong north-westerly ‘Mistral’ winds (MEDOC-group, 1970) initiates an intensification of the basin’s cyclonic circulation, which causes a shallowing of the pycnocline from a usual depth of approximately 200-250 m (Perkins and Pistek, 1990) to < 100 m (see Rohling et al., 1995).

The preconditioning phase is followed by a phase of violent mixing. Throughout February, the density of surface waters increases due to cooling and intense evaporation (2 cm day^{-1} ; MEDOC-group, 1970), eliminating the gradient between the surface and intermediate waters. This results in “chimneys” of convective mixing that reach throughout the water column to great depths (>2000m), developing within the centre of the gyre (MEDOC-group, 1970; Leaman and Schott, 1991). Incidentally, the existence of discrete “chimneys” of deep convective mixing was observed for the first time in this area during the MEDOC study, and similar features have since been recognised in other areas of deep water formation (notably the Norwegian Sea). The geographical extent of the region of deep-water formation is characterised at the surface by high salinities (38.4 p.s.u.) mixed up from below, from the intermediate water (MEDOC-group, 1970).

Then follows a phase of sinking and spreading. As the stormy period ceases, the mixed water sinks rapidly to form WMDW (Figure AA). The newly formed watermass is characterised by a relatively high oxygen content ($4.4 - 4.7 \text{ ml l}^{-1}$), and spreads horizontally between 1500 and 3000 m into the Balearic basin and Tyrrhenian Sea (Wüst, 1961). On entering the Alboran Sea, WMDW forms a narrow (~ 20 km) boundary current flowing westward along the Moroccan coast before entering the Strait of Gibraltar. In the Alboran Sea WMDW reaches speeds of approximately 5 cm s^{-1} , and it contributes an estimated 0.3 Sv (25%) to the outflow over the Gibraltar Sill (Parrilla et al., 1986; Richez and Gascard, 1986).

3.4.2. Eastern Mediterranean Deep Water (EMDW)

Throughout the period of oceanographic observation, until the late 1980s-early 1990s, the Adriatic Sea was found to be the main source area of EMDW formation (Pollak, 1951; Wüst, 1961; Malanotte-Rizzoli and Hecht, 1988; POEM-group, 1992). In winter, cold and dry north-easterly winds (Bora) cause intense cooling of the North Adriatic shelf waters (Ozsoy, 1981), which are of relatively low salinity due to dilution with fresh water from the Po river. The resultant cold waters flow towards the deep south Adriatic Basin, where mixing occurs with the warmer but more saline MIW that penetrates the South Adriatic across the Otranto Sill. The mixing of the cold and relatively low-salinity shelf waters with warm and highly-saline MIW results in the formation of Adriatic Deep water (ADW). Although ADW has a lower salinity (< 38.7‰) than MIW, it is also cooler, with values between 13.0 and 13.6°C. The resultant higher density of ADW allows it to settle below the MIW down to the greatest depths in the eastern Mediterranean basin (in any case, it used to do so until the late 1980s-early 1990s). It thus forms a major component of the EMDW. The EMDW circulates in a deep western boundary through the Ionian Sea before entering into the Levantine Basin (POEM-group, 1992). Roether and Schlitzer (1991) constructed a 22-box model for the deepwater flow in the Ionian and Levantine basins. Their results indicate that the thermohaline circulation in the eastern Mediterranean at that time consisted of a single vertical cell through both basins, driven by Adriatic deepwater formation. The derived rate of deepwater supply from the Adriatic Sea into the eastern Mediterranean was 0.29 Sv and the turnover time about 126 years (POEM-Group, 1992).

The importance of the Aegean Sea as a contributor to EMDW ventilation has been intensely debated. Pollak (1951) rejected the hypothesis that the Aegean Sea is a

source of deepwater formation, arguing that the Adriatic is the only source. Wüst (1961) disagreed, stating that the Aegean Sea source may be minor but not negligible. Indeed, Miller (1963) reported evidence that Aegean Deep Water (AeDW), contributing to the EMDW, formed sporadically in the Aegean Sea before flowing into the Levantine Basin via the Straits of Kasos and Karpathos. Roether et al. (1983), however, concluded from ^3H and ^3He data that the bottom waters of the Eastern Mediterranean were formed exclusively in the Adriatic. The entire debate took a dramatic turn when observations obtained on *RV Meteor* cruise M31-1 (January–February 1995) reported that an influx of Aegean Sea water had replaced approximately 20% of the deep and bottom waters of the eastern Mediterranean, strongly enhancing the observed deep/bottom-water salinities and displacing older waters upwards (Roether et al., 1996). It was inferred that Aegean Sea outflow now contributed up to 65% to the deep and bottom waters of the Eastern Mediterranean (Roether et al., 1996).

Circulation in the Aegean Sea is mainly controlled by the regional climate, local riverine inputs that occur mainly in winter, and the Black Sea surface-water outflow that increases in summer (Poulos et al., 1997). Annual surface temperatures in the Aegean Sea vary from <13 °C in winter to >24 °C in summer. Salinity varies from <31.0 to >39.0 p.s.u. (Poulos et al., 1997), with locally lowest values (26 p.s.u.) in summer as a result of the Black Sea outflow (Yüce, 1995). The formation of Aegean Deep Water (AeDW) is again closely related to the influences of salty Levantine Intermediate Water. As the LIW-derived Aegean Intermediate Water (AeIW) travels north along the Turkish Coast, the prevailing offshore winds cause its upwelling to the surface (Lascaratos 1989; Yüce 1995). In these shallow eastern shelf areas, the AeIW consequently forms a single uniform watermass from the surface to the sea floor. As the upwelled AeIW progresses northwards at the surface, it is directly affected by the regional climate. Winter-time cold and dry northerly outbreaks of polar/continental air masses cause strong surface buoyancy loss from the Aegean Sea, through cooling and increasing salinities (Theocharis and Georgopoulos, 1993). This leads to the formation of AeDW, which today fills the Aegean Basin below 300m (Bruce and Charnock, 1965; Burman and Oren, 1969; Miller et al., 1970; Miller, 1972; Theocharis, 1989; Yüce, 1995).

As stated before, AeDW formation was long considered of minor importance to the deepwater ventilation of the open Eastern Mediterranean, but recent studies show that specific (cold) climatic forcing over the Aegean in the early 1990s caused higher-salinity AeDW to replace Adriatic Deep Water (ADW) as the dominant deep water in the open Eastern Mediterranean [Roether et al. 1996, Samuel et al. 1999; Klein et al., 1999]. This event, which has been named the “Mediterranean Transient” initiated a new mode of deep ventilation in the eastern Mediterranean basin that has persisted until today (B. Klein, pers. comm. Nice, April 2004).

4. Quaternary climatic and hydrographic changes

The Quaternary Mediterranean palaeoclimatic and palaeoceanographic history reveals marked variability with both orbital (“Milankovitch”) and so-called “sub-orbital” or “sub-Milankovitch” periods. The former refers to variability with periods similar to those of the astronomical cycles of eccentricity, obliquity and precession. The latter

refers to variability at periods shorter than those of the astronomical cycles (i.e., shorter than 19,000 years).

The astronomical cycles (eccentricity with periods of ~400 and ~100 kyr, obliquity with a main period of 41 kyr, and precession with periods of 23 and 19 kyr) govern changes in the intensity and distribution of insolation. They have especially important impacts on glacial-interglacial alternations and monsoon intensity. The Pleistocene glacial-interglacial cycles followed first obliquity and then (since ~900 ka BP) eccentricity time scales. Typical glacial-interglacial contrasts in the Mediterranean's climatic and oceanographic features are well illustrated by a comparison of the Last Glacial Maximum with the current and previous interglacial maxima. Superimposed on the glacial-interglacial cycles, frequent episodes of organic-rich sediment accumulation have occurred in the (eastern) Mediterranean, timed according to monsoon maxima as determined by the eccentricity-modulated precession cycle.

So-called sub-Milankovitch climate variability is globally widespread as well, but its origin remains elusive. The millennial-scale “Dansgaard-Oeschger events” were first observed in temperature proxy records from the well-dated Greenland ice cores (Langway et al., 1985; Dansgaard et al., 1993; Grootes et al., 1993), and now provide a widely accepted template for sub-Milankovitch variability of the last 110 kyr in the North Atlantic-Eurasian region (e.g., Broecker, 2000; Voelker et al., 2002; Rohling et al., 2003; Hemming, 2004; and references therein). Notable “tie-points” are associated with the extreme cold events known as “Heinrich events”, when massive ice-berg flotillas caused a great pulse of ice-raftered debris deposition and melt-water flooding in the North Atlantic, with cold and arid climatic effects that were noted on an at least northern hemispheric scale (see overviews in Rohling et al., 2003; Hemming, 2004). The Mediterranean sedimentary record contains ample evidence of millennial to centennial time-scale sub-Milankovitch variability that has been convincingly related to this template.

In the following sections, we will first introduce relevant aspects of orbital forcing, followed by overviews of: (a) the character of glacial-interglacial cycles in the Mediterranean; (b) the impact of insolation-driven monsoon maxima on Mediterranean hydrography and sedimentation; and (c) the expressions of centennial-to millennial-scale variability in the basin.

4.1. The orbital periods and insolation at 65°N

In the 1860-1870s, James Croll pioneered an astronomical theory of climate change. In the late 1930s, the Serbian engineer Milutin Milankovitch expanded this theory, calculating the astronomically determined fluctuations in the intensity and distribution of solar radiation onto the earth, presented in the form of insolation reconstructions for various discrete latitude bands. This section briefly introduces the astronomical cycles, starting with eccentricity and precession, and concluding with the obliquity or tilt cycle.

First, it is useful to summarise the nature of the cardinal points in the seasonal cycle. On an annual time scale, the position of the earth's rotational axis, tilted relative to the plane of the earth's orbit around the sun, is fixed in space. Today, the North Pole points towards the star Polaris. Northern hemisphere winter starts with the northern

hemisphere (“boreal”) winter solstice, when the North Pole lists directly away from the sun, resulting in the shortest day on the northern hemisphere. Next, the boreal spring (“vernal”) equinox marks the start of boreal spring. During an equinox, the boundary between the illuminated and dark half-globes passes through both Poles, so that day and night have identical durations at all points of the world. Then follows the boreal summer solstice, when the North Pole lists directly towards the sun, resulting in the longest day on the northern hemisphere. It marks the start of boreal summer. Thereafter, the boreal autumnal equinox is reached, which marks the start of boreal autumn.

Eccentricity concerns the shape of the earth’s orbit around the sun, which varies from near circular to distinctly elliptical. An ellipse has two focal points, and as the ellipse transforms to a circle, the two focal points approach one another. Eccentricity is expressed as a measure of the distance between the two focal points relative to the distance along the long axis of the ellipse. The eccentricity of the earth’s orbit varies between almost 0 and about 6%. The sun occupies one of the focal points of the earth’s orbit, the other one is empty. The non-circular shape of the orbit dictates that earth passes a point nearest the sun (“perihelion”) and a point furthest away from the sun (“aphelion”) during each of its annual revolutions around the sun. Today, perihelion occurs close to the boreal winter solstice, and aphelion close to the boreal summer solstice. Note that, when the orbit is near circular – an eccentricity minimum – the earth’s distance to the sun is virtually constant through the year. The eccentricity of the earth’s orbit changes in a cyclic fashion, with three main periods: 94,800 years, 123,800 years, and 404,000 years. Palaeoclimate studies commonly approximate these with apparent periods of 100,000 and 400,000 years. The impact of eccentricity on insolation is primarily through modulation of the effects of precession.

Precession refers to the fact that the earth’s rotational axis relative to its orbital plane is not fixed in space, but displays a long-term wobble, similar to the axis of a spinning top. This changes the direction of the axis in space, so that the earth’s North Pole, which today points towards Polaris, points towards Vega after half a precession cycle, and back towards Polaris again after a complete precession cycle. A full precession cycle takes 26,000 years, but due to other complications in the earth-sun motions (the entire earth orbit itself slowly rotates around the sun about once for every four precession periods) the precession cycle manifests itself in insolation with two dominant periods: one around 23,000 years and the other around 19,000 years.

Precession causes a very slow shifting of the dates of the solstices and equinoxes along the orbit. A quarter of a cycle ago (about 5,500 years BP), therefore, perihelion occurred near to the boreal autumnal equinox. Half a cycle ago (about 11,000 years BP), perihelion occurred close to the boreal summer solstice. Three quarters of a cycle ago (about 16,500 years BP), perihelion coincided with the boreal vernal equinox, and a full cycle ago the situation concerning precession was similar to the present. The climatic impacts of the precession and eccentricity cycles need to be viewed together. Today, in its slightly elliptical orbit, the earth is at perihelion around the boreal winter solstice (3 January and 21 December, respectively). It is at aphelion around the boreal summer solstice (4 July and 21 June, respectively). When the orbit approaches a circle, these distance differences would have negligible effects. However, since some eccentricity applies, the solar radiation on illuminated places of the globe will be somewhat more intense in boreal winter (austral summer) than in boreal summer

(austral winter). This weakens the seasonal contrast on the northern hemisphere, and strengthens it on the southern hemisphere. The precession cycle then shifts the distribution of the seasons around the elliptical orbit. Half a precession cycle ago, perihelion occurred near the boreal summer solstice and aphelion around the boreal winter solstice, which enhanced the seasonal contrast on the northern hemisphere.

The cycle of obliquity concerns changes in the angle of the earth's rotation axis relative to the perpendicular of the plane of the earth's orbit over a period of 41,100 years, between 22.5 and 24.5 degrees. Today, the angle is about 23.5 degrees, so that the sun during the boreal summer solstice stands directly overhead at about 23.5° North latitude. This represents the maximum North latitude where the sun at any one time in the year reaches a directly overhead position – the Tropic of Cancer. During the boreal winter solstice (austral summer solstice) this condition is reached at about 23.5° South latitude – the Tropic of Capricorn. On a perfectly spherical earth, the obliquity cycle would therefore shift the position of the Tropics between 22.5 and 24.5° latitude (the actual values are 22.04 and 24.45°). In addition, the obliquity (or “tilt”) of the axis affects the amount of sunlight received at the high polar latitudes. For strong tilt, the poles receive more sunlight, and the sun's rays also reach the polar surface at a higher angle, which both increases the energy received per unit area and decreases reflection.

Variations in the astronomical parameters have now been reliably calculated back to 10-15 Ma or so (Laskar et al., 1993; Laskar, 1999). Although many studies discuss palaeoclimatic records in terms of changes in the individual orbital parameters, the majority concentrates on their combined influence on insolation changes in specific latitude bands. Particular interest concerns the insolation changes at 65 degrees North latitude. At this latitude, earth is occupied by great landmasses, which causes a sensitive setting for responses to insolation. Astronomically-determined insolation records have been used as a template for glacial-interglacial variations reflected in marine stable oxygen isotope series (e.g., Imbrie et al., 1984, 1992; Martinson et al., 1987), and for variability in the northern hemisphere's Indian/Asian and African monsoon systems through time (among others, Rossignol-Strick, 1983; 1985; Hilgen, 1991a,b; Hilgen et al., 1993, 1995; Lourens et al., 1992, 1996, 2001; Prell and Kutzbach, 1987; Shimmield et al., 1990; Clemens and Prell, 1991; Clemens et al., 1996). Because the insolation series is accurately calculated from astronomical changes with time, correlations of palaeoclimate records to the insolation records offer a sound insight into the chronology of the records. This concept lies at the heart of so-called “astronomical or orbital tuning” of the geological time-scale. Great advances have been made in the development of an astronomically-tuned geochronology, both on the basis of deep-sea stable oxygen isotope variations (e.g., Imbrie et al., 1984, 1992; Martinson et al., 1987; Pälike and Shackleton, 2000), and on the basis of Mediterranean sapropel occurrences, other lithological alternations, and stable isotope data (e.g., Hilgen, 1991a,b; Hilgen et al., 1993, 1995; Lourens et al., 1992, 1996, 2001).

4.2. Glacial cycles in the Mediterranean

The major glacial / interglacial climate oscillations of the Pleistocene had large impacts on the Mediterranean environment ([Chapters 5 and 7](#)). Development of a fixed anticyclone over the north European ice sheet and colder sea surface

temperatures during glacial times are thought to have resulted in colder and drier conditions (i.e., reduced moisture supply from colder air masses) (Rognon, 1987), with a likely increased seasonality of precipitation over the Mediterranean (Prentice et al., 1992). The present climate conditions are characterised by a high interglacial sea-level position, relatively dense vegetation cover, relatively high infiltration rates, and moderate river discharges, as summarised for the western Mediterranean by Rose et al. (1999). Glacial times, in contrast, were characterised by a low global sea level, open vegetation with large areas of bare ground and unconsolidated sediments, soils affected by high physical stresses and highly peaked river-discharge regimes (Rose et al., 1999). Past vegetation (pollen) and lake-level records confirm the contrast between generally warm and relatively humid interglacial conditions and cold, relatively arid glacial conditions in the Mediterranean basin (e.g., Wijmstra et al., 1990; Digerfeldt et al., 2000; Elenga et al., 2000; Magri and Parra, 2002; Tzedakis, 1993, 1999; [Chapter 5](#)). Also, wind-blown dust transport into the Mediterranean was high during glacial times, suggesting enhanced aridity (Dinarès-Turell et al., 2003; Larrasoña et al., 2003; [Chapter 19](#)).

The most robust palaeoenvironmental characteristic of the last glacial maximum (LGM, ~20 thousand years ago; ka BP) is a global sea-level low-stand at 120 or 125 m below the present-day level (Fairbanks, 1989, 1990; Rohling et al., 1998; Siddall et al., 2003; Peltier, 2004). This lowering had serious impacts on Mediterranean hydrography, due to its effect on the hydraulically controlled exchange of watermasses through the Strait of Gibraltar. Any such sea-level lowering would cause a severe reduction in the exchange transport (to roughly half the modern value; Rohling and Bryden, 1994; Rohling, 1994; Myers et al., 1998; Matthiessen and Haines, 2003). This would increase the residence-time of waters within the Mediterranean basin (calculated as Volume/Flux out), causing longer exposure of Mediterranean waters to the strong net evaporation, which leads to a considerable increase in salinity (stable oxygen isotope data substantiate the impact of this concentration effect, see below) ([Figure 9a](#)). Any subsequent climatic amelioration associated with sea-level rise would cause a rapid reduction in salinities within the basin, which would be conducive to poor deepwater ventilation (Rohling, 1994; Matthiessen and Haines, 2003).

The lower glacial sea-level position is also thought to have caused a shoaling of the density gradient (pycnocline) between intermediate and surface waters within the Mediterranean, with impacts on the plankton community structure by supporting a widespread deep chlorophyll maximum (Rohling and Gieskes, 1989; Rohling, 1991a; Rohling and Bryden 1994; Myers et al., 1998). The aforementioned glacial concentration effect would furthermore have enhanced the salinity contrast between the Mediterranean and the open ocean, and so between outflow and inflow through the Strait of Gibraltar. Effectively, the Mediterranean outflow flux would have been reduced, but its density contrast with ambient Atlantic waters would have been significantly enhanced, resulting in a deeper-settling, smaller-volume glacial Mediterranean Outflow plume in the Atlantic (e.g., Rohling, 1997). Similar impacts of sea-level lowering apply to other concentration basins, such as the Red Sea (e.g., Rohling and Zachariasse, 1996; Rohling et al., 1998a; Siddall et al., 2003; and references therein).

The contrast between glacial and interglacial conditions in the Mediterranean is particularly obvious when comparing Sea Surface Temperature (SST) reconstructions for the LGM with those for the most recent, Holocene, Climate Optimum (HCO, 9-6 ka BP), the time when the most recent sapropel was deposited ([Figure 10](#)). The reconstructions are based on analysis of abundance data of planktonic foraminifera ([Plate 1](#)) from sediment cores with a recently-developed Artificial Neural network method to derive Mediterranean temperature values (Hayes et al., 2005). On a basin-wide scale, these reconstructions corroborate the basic SST assumptions that were used previously in modelling studies (Myers et al., 1998).

Complementary information on changes in the net freshwater budget between the LGM and HCO may be obtained from analysis of spatial patterns in stable oxygen isotope values through the basin (Kallel et al., 1997a,b; Rohling and de Rijk, 1999a,b and references therein). The stable isotope data can be used to assess changes in salinity, subject to significant caveats (Rohling 1999a; Rohling et al., 2004). Myers et al. (1998) used the isotope distributions to infer idealised LGM and HCO distributions of sea surface salinity (SSS) for use as restoring boundary conditions in his modelling experiments of Mediterranean palaeocirculation. Overall, such studies suggest that net evaporation from the Mediterranean during the LGM may not have been very different from the present, suggesting that any reduced effective moisture supply from colder air masses was approximately offset by reduced evaporation from a colder sea. The higher LGM-Present salinity contrast in the Mediterranean, relative to that in the open ocean, appears to be dominated by the glacial concentration effect (i.e., the impact of 120-125 m glacial sea-level lowering on watermass exchange through the 284-m deep Strait of Gibraltar).

4.3. Monsoon maxima and Mediterranean sapropels

Sapropels are dark, often laminated, organic-rich sediments found intercalated between with the normal, organic-poor, hemipelagic sediments throughout the entire eastern Mediterranean. There are rare examples also from the western Mediterranean, especially from Pliocene times. Sapropels range from a few millimetres to more than a metre in thickness, and have been deposited intermittently throughout the Neogene and Quaternary (among countless others: Kullenberg, 1952; Olausson, 1961; Van Straaten, 1972; Cita et al., 1973, 1977; Vergnaud-Grazzini et al., 1977; Thunell et al., 1977, 1983; Stanley, 1978; Williams et al., 1978; Cita and Grignani, 1982; Rossignol-Strick et al., 1982; Rossignol-Strick, 1983; Vergnaud-Grazzini, 1985; Rohling and Giekens, 1989; Emeis et al., 1991, 1998, 2003; Hilgen, 1991a,b; Hilgen et al., 1993, 1995; Rohling, 1994; Van Os et al., 1994; Lourens et al., 1992, 1996, 2001; Nijenhuis et al., 1996; Rohling, 1999b (edited volume); Meyers and Negri, 2003 (edited volume); and contributions and references therein).

Sapropels are commonly marked by an absence of benthic foraminifera, and are preceded by a short interval containing benthic faunas indicative of severe bottom-water oxygen depletion (such faunas sometimes return within, or persist into/through, the sapropel) (e.g. Van Straaten, 1972; Nolet and Corliss, 1990; Verhallen, 1991; Rohling et al., 1993b, 1997; Nijenhuis et al., 1996; Jorissen, 1999; Mercone et al., 2001; Casford et al., 2003; Schmiedl et al., 2003). In marine cores, sapropels are recognisable as beds ranging in colour from dark grey to olive green and black. Exposed in land-sections, sapropels appear in notably darker shades of grey than

surrounding beige to blue clays, and commonly weather into distinct reddish-brown hues. Sapropels may display remarkably well-preserved lamination. *Include photo of Meteor 152.* The shallowest reported occurrence of the four youngest (most cored) sapropels in the open eastern Mediterranean is ~300 m (Shaw and Evans, 1984; Rohling and Gieskes, 1989; Rohling et al., 1993a). In the Adriatic Sea, the upper depth limit seems to have been at a deeper level, below 400 m (Jorissen et al., 1993). In the Aegean Sea, sapropels are found up to 120 m water depth (Perissoratis and Piper, 1992; Casford et al., 2002).

Following almost six decades of research on Mediterranean sapropels since their initial discovery in marine sediment cores recovered during the Swedish Deep-Sea Expedition of 1946-47, a general (but not unanimous) consensus has emerged that sapropels were formed during times with a combination of (a) enhanced abundances of organic matter sinking from surface waters (i.e., export production), and (b) reduced deepwater ventilation due to diminished excess evaporation from the Mediterranean basin caused by enhanced freshwater discharge (for overviews, see: Cita and Grignani, 1982; Rohling, 1994; Emeis et al., 1998; Cramp and O'Sullivan, 1999; Rohling et al., 2004). These impacts will be discussed below, and are summarised in [Figure 11](#) (modified after Rohling, 1994).

Evidence for elevated export production has been compiled through a combination of proxy data that includes phyto- and zoo-plankton abundances, stable isotope gradients, organic-carbon accumulation and composition, and Ba/Al ratios in the sediment (among many others: Cita and Grignani, 1982; Rohling and Gieskes, 1989; Castradori, 1993; Higgs et al., 1994; Thomson et al., 1995, 1999; Van Os et al. 1995; Kemp et al., 1999; Mercone et al., 2000, 2001; Rohling et al., 2004). Productivity increases during the deposition of sapropels appear to have been of a (temporally integrated) basin-wide nature, especially in the form of a Deep Chlorophyll Maximum (Rohling and Gieskes, 1989; Castradori, 1993; Rohling, 1994; Kemp et al., 1999; Corselli et al., 2002), although on shorter time-scales there may have been considerable spatial “patchiness” (Casford et al., 2003). The development of a Deep Chlorophyll Maximum with high export production at sapropel times has been ascribed to hydrographic re-arrangements in response to the decrease in buoyancy loss from the Mediterranean at times of enhanced freshwater input. Notably, the reduced surface buoyancy loss is thought to have caused a shoaling of the surface-intermediate water interface from its present depth below the zone of light penetration (euphotic zone) to a depth within the euphotic layer (Rohling and Gieskes, 1989; Rohling, 1991b, 1994; Myers et al., 1998). This would allow nutrients stored within the subsurface waters to become utilised for production at the base of the euphotic layer. There is a continuing debate about the ultimate supply of the nutrients that could have supported extensive organic carbon burial in the sediments. Early work concentrated on riverine nutrient input at times of sapropel deposition, but biogeochemical modelling suggests that river-input would be insufficient if the nutrient budget were at steady state during sapropel formation (Stratford et al. 2000). However, recent work has suggested that the basin may have accumulated nutrients over as much as 1500 years prior to the onset of organic carbon burial, so that the nutrient budget during sapropel deposition ought to be considered as a product of accumulation over much longer time scales, and so was not at steady state (Casford et al., 2002).

Strong evidence for enhanced freshwater influx into the eastern Mediterranean at sapropel times comes from negative anomalies in stable oxygen isotope ratios measured on the calcium-carbonate shells of planktonic foraminifera that live in near-surface habitats. Fresh water has distinctly low oxygen isotope ratios compared with sea water, and especially the fresh waters derived from heavy (monsoon-type) rainfalls are isotopically very light. Admixture of freshwater floods to the Mediterranean surface waters therefore causes light isotope anomalies in the surface-dwelling foraminifera (e.g., Vergnaud-Grazzini et al., 1977; Thunell and Williams, 1983, 1989; Jenkins and Williams, 1984; Ganssen and Troelstra, 1987; Kallel et al., 1997a,b; Tang and Stott, 1991; Rohling and De Rijk, 1999a,b; Emeis et al., 1998, 2000, 2003; Rohling et al. 2004). Sedimentary Ti/Al ratios, palaeomagnetic data, and clay mineralogical studies confirm that times of sapropel deposition were characterised by humid climates with high runoff, whereas intervening times were arid with reduced riverine and enhanced wind-blown sediment supply (e.g., Krom et al., 1999; Foucault and Mélières, 2000; Wehausen and Brumsack, 2000; Lourens et al., 2001; Larrasoña et al., 2003).

A particularly relevant discovery concerned the temporal coincidence between sapropel occurrences and insolation-driven monsoon maxima, affecting the eastern Mediterranean via changes in Nile discharge (Rossignol-Strick et al., 1982; Rossignol-Strick, 1983, 1985). These authors approached the problem by specifying an index for monsoon intensity (“monsoon index, M”) as a function of two parameters, namely insolation at the (north) Tropic of Cancer (I_T), and the insolation difference between the Tropic of Cancer and the equator ($I_T - I_E$), so that $M = 2I_T - I_E$. The variation in the index value was considered relative to the value of AD 1950 (Rossignol-Strick, 1985). This pioneering work instigated an intensive search into the timing of sapropel formation over their full temporal range, which confirmed that sapropels were always formed at times when perihelion falls in boreal summer (“precession minima”, relative to “maxima” that represent the present configuration with perihelion in boreal winter). It was also observed that not all precession minima have sapropels, but that they instead occur in discrete clusters. Each cluster was found to represent times of maximum orbital eccentricity, in agreement with eccentricity modulation of the impact of precession (Hilgen, 1991a,b; Hilgen et al., 1993, 1995; Lourens et al., 1996, 2001) (Figure 12). Numerical climate modelling corroborated the impact of precession and eccentricity on monsoon intensity (e.g., Kutzbach, 1985; Kutzbach and Guetter, 1986; COHMAP, 1988).

In essence, insolation changes affect the monsoons as follows. Air rises over a hot surface, giving low surface pressure, while it descends over a cool surface, giving high surface pressure. Because land has much lower thermal inertia than ocean, land surfaces experience a much stronger annual fluctuation in both temperature and pressure than ocean surfaces. During periods with enhanced seasonal insolation contrasts, the higher summer insolation increases surface temperatures especially over land, and this in turn amplifies the atmospheric pressure differences between land and sea. In addition to this direct radiative forcing, the preceding winter conditions also play a role, due to the thermal inertia of the ocean. The slow response of oceanic temperatures on seasonal time scales amplifies the land-sea temperature contrast from direct solar heating, and thus enhances the land-sea pressure differences. In summer, the strong land (low) to sea (higher) pressure difference leads to surface air flow from ocean to land. This air flow is moisture laden, because of evaporation over the ocean.

The air expands and cools as it rises over the land, a process that is accelerated if the air masses are forced up by mountain ranges. The cooling causes the air-masses to shed their vapour as rain. Condensation releases heat, which amplifies the process by enhancing the ascending motion in the air column. Thus, a zone develops of high-frequency and high-intensity monsoonal rains.

We emphasise that the above description of the summer monsoon in terms of surface thermal forcing (i.e., as a super sea-breeze) represents a strongly simplified generalisation. In reality, the low pressure cell over land derives much of its intensity and continuity from dynamical effects related to the mean high-level wind flow in the atmosphere (at the 500 millibar level, or approximately at 5.5 km height), especially in the case of the Indian/Asian monsoon. As an extra complication, it is thought that the strength of the trade winds on the opposite (winter) hemisphere may determine a ‘push’ across the equator into the summer monsoonal low. Despite its schematic nature, however, the thermal concept offers reasonable representation of the general features of the African monsoon. Over Africa, the axis of low pressure at the surface (‘the monsoonal low-pressure trough’) follows the seasonal march of the sun at its high point (zenith), which reaches the Tropic of Cancer at the summer solstice. This seasonal swing over the band of monsoon-influenced latitudes in Africa can be smooth because most of Sahelian and Saharan North Africa is relatively flat. The influence of ‘push’ effects by the southern (winter) hemisphere trade winds on the North African summer monsoon was accounted for in the monsoon intensity calculations of Rossignol-Strick and co-workers by inclusion of an austral winter insolation gradient (G_s) between 20 and 70°S, so that $G_s = I_{20} - I_{70}$ (Rossignol-Strick, 1985).

Within the context of monsoon intensification, it is relevant to briefly review reconstructions of the Nile and the Sahara since the LGM, as summarised by Adamson et al. (1980) and Williams et al. (2000). These authors report that, from the LGM until roughly 12,500 years BP, Nile discharge was very low. The White Nile was a seasonal, intermittent river until ~12,500 years BP, when Lake Victoria overflow developed and the “buffering” Sudd swamps in Sudan became established, which ensured a more regular, perennial discharge from the White Nile. From ~12,500 years BP, there was an (intermittent) period with very high discharge, associated with the early-mid Holocene monsoon maximum that developed during the insolation maximum of that time. This maximum ended with a development towards generally much drier conditions around 5000 years BP, heralding the development of the modern Nile regime. These trends are supported by general findings that astronomical forcing affects not only the intensity of the African monsoon, but also its spatial influence, causing strong reductions in the size of the Sahara desert by northward migration of its southern margin.

The so-called “greening” of the Sahara is a well-known response in numerical climate models that include vegetation-climate feedback mechanisms (Brovkin et al., 1998; Claussen et al., 1998). The concept is supported by a wide variety of field observations: rock-art and animal, human and vegetation remains in the central Sahara; massive expansion of Lake Chad; presence of substantial palaeolakes in currently hyperarid areas such as the Oyo depression of NW Sudan; and activation of large-scale systems of presently inactive wadis (e.g., Pachur and Braun, 1980; Gaven et al., 1981; Ritchie et al., 1985; McKenzie, 1993; Szabo et al., 1995; Petit-Maire and

Guo, 1997; Pachur 2001; Gasse, 2000, Hoelzmann et al., 2000; Williams et al., 2000; Mandel and Simmons, 2001; Hassan, 2002 (edited volume); and many references therein). A recent study suggested on the basis of stable oxygen isotope data that the monsoon front penetrated sufficiently far northwards during the insolation maximum of the previous interglacial maximum to have caused significant precipitation to the North of the central Saharan watershed (~21°N) (Rohling et al., 2002b). In that case, significant runoff would not only have reached the eastern Mediterranean via the Nile River, but also along the wider North African margin. A study concerned with aeolian dust variations over the last 3 million years supported that scenario for all substantial insolation maxima (Larrasoña et al., 2003). Archaeological observations around exclusively rain-fed depressions on the Libyan Plateau suggest that monsoonal summer rains of central Africa periodically penetrated at least as far north as Kharga (roughly 25°N) during the early-mid Holocene, despite the fact that conditions during that pluvial phase seem to have remained drier than during earlier Quaternary pluvial phases (Mandel and Simmons, 2001).

The observation of Mandel and Simmons (2001) that the Holocene monsoon maximum was of a relatively low intensity, compared with previous Quaternary monsoon maxima, has been corroborated by recent work to quantify the Holocene and previous interglacial (Eemian) monsoon impacts on the freshwater budget of the eastern Mediterranean (Rohling, 1999; Rohling et al., 2004). Eastern Mediterranean surface-water oxygen isotope ($\delta^{18}\text{O}$) data show two very distinct “peaks” in the Eemian monsoon maximum, separated by an “interruption” that lasted about 800 years. A mixed-layer $\delta^{18}\text{O}$ box model to quantify freshwater flooding during the two Eemian monsoon peaks suggests that the basin-averaged Mediterranean excess of evaporation over freshwater input was reduced to 5-45% (older peak) and 35-60% (younger peak), relative to the present (Rohling et al., 2004). It also suggests that the “interruption” between the two peaks was characterised by excess evaporation at levels very close to present-day values. Using a similar technique, the excess evaporation during the early-mid Holocene monsoon maximum was estimated at about 65% of the present value (Rohling, 1999). Using a different technique, based on an ocean general circulation model (OGCM), Myers (2002) suggests that the excess evaporation value for the Holocene monsoon maximum ranged below 80% and most likely around 20-40% of the present-day value. As yet, eastern Mediterranean $\delta^{18}\text{O}$ records through the Holocene monsoon maximum have revealed only weak indications of a monsoon “interruption”, but neodymium (Nd) isotopes seem more conclusive that such an interruption did occur during the Holocene (Scrivner et al., 2004). African lake levels also clearly demonstrate an arid interlude, dated between about 8.5 and 7.8 ka BP (Gasse, 2000), coincident with a cooling event of ~500 year duration over the Aegean and Adriatic Seas (see, for example, Rohling et al., 2002a).

Not only the monsoon system was intensified at times of sapropel deposition. Records of pollen and spore abundances from terrestrial vegetation suggest high abundances of species that require wet summers around the Northern Borderlands of the Eastern Mediterranean (NBEM) at times of sapropel formation (Rossignol-Strick, 1987, 1995; Wijmstra et al., 1990; Rohling and Hilgen, 1991; Tzedakis, 1993; Mommersteeg et al., 1995; Frogley et al., 1999). Winter precipitation is thought to have been increased in the NBEM as well (Wijmstra et al., 1990). Isotope studies on speleothems corroborate the inferred increase in precipitation (Bard et al., 2000; Matthews et al., 2000; Bar-Matthews et al., 1999; 2000; 2003), as do elevated lake levels (e.g.,

Digerfeldt et al., 2000). The conditions at times of sapropel formation would therefore appear to have been considerably different from the typical dry-summer climate that characterises the area today. Direct precipitation from the African and Indian monsoon systems is unlikely to have penetrated into the Mediterranean basin, demonstrating that the moisture for precipitation in the NBEM derived from regional processes, likely in the form of Mediterranean depressions (Rohling and Hilgen, 1991). This notion was corroborated by isotopic characteristics of speleothems in Soreq Cave, Israel, which demonstrate a local Mediterranean moisture origin (Matthews et al., 2000; Bar-Matthews et al., 2003).

The summer flux of Mediterranean moisture at times of insolation maxima even affected the northernmost tip of the Red Sea, where it has been described as the “Mediterranean monsoon” (Arz et al., 2003). Importantly, this process would not likely have affected the Mediterranean Sea’s overall hydrological budget very significantly – although any precipitation would have led to runoff into the basin, the original evaporative loss took place from the same basin. Any transport into another basin’s watershed area (e.g., the Red Sea, Jordan Valley and Dead Sea, or Tigris/Euphrates and Persian Gulf) would imply that the regional “humidity” in the NBEM might even have coincided with a slight increase in net evaporative loss from the Mediterranean. Importantly, however, the process would reflect considerable fresh-water redistribution in a generally eastward direction within the Mediterranean basin, so that the hydrological budget may have been substantially affected on local scales and in terms of regional gradients.

The (especially monsoon-related) reduction of Mediterranean excess evaporation would have caused a reduction in the salinity of newly formed intermediate water. Numerical modelling suggests that intermediate-water formation is likely to have shifted from a normal salt-dominated LIW mode, to a temperature-dominated mode driven from the Adriatic Sea at times of sapropel formation (Myers et al., 1998; Myers et al., 2002). Stable isotope data for planktonic foraminiferal species with different depth habitats from the Aegean Sea corroborate that notion (Casford et al., 2002). The collapse of the first, salt-driven, stage of the deep-ventilation “motor” would have caused any new deep water to form at much lower salinities (hence, lower densities) than it did in times before the monsoon intensification (Rohling 1994; Myers et al. 1998; Myers, 2002). Thus, newly formed deepwater masses could not displace the existing, denser, “old” deep waters (ODW) formed before the fresh-water flooding. As a result, the ODW became poorly ventilated, and eventually oxygen depleted due to continuing remineralisation of sinking organic matter (for overview, see Rohling, 1994). At least down to ~2000 m depth some occasional ventilation may have persisted during the deposition of several sapropels, and down to those depths the occurrence of truly anoxic conditions likely was restricted to spatially discontinuous “blankets” over the sea-floor topography (Casford et al., 2003).

4.4. Centennial- to millennial-scale variability

As mentioned previously, deep ventilation in the Mediterranean basin is strongly affected by winter-time, orographically channelled, northerly outbursts of cold polar and continental air over the northern sectors of the basin. Fluctuations in the intensity and frequency of such events are also reflected in temperature proxy data. Terrestrial and marine Mediterranean palaeoclimate and palaeoceanographic proxy records that

are resolved on centennial time scales have been found to reflect multi-centennial to millennial fluctuations (Rohling et al., 1998b, 2002a,b, 2004; Paterne et al., 1999; Cacho et al., 1999, 2000, 2001, 2002; Allen et al., 2000; Combourieu-Nebout et al., 2002; Sanchez-Goñi et al., 2002; Tzedakis et al., 2004). These have often been related to climatic oscillations in the wider North Atlantic realm by correlation with the ice- $\delta^{18}\text{O}$ records and non-sea-salt ion series (dust) from the well-dated GISP2 and GRIP ice cores (Greenland summit). Particularly strong cooling events have been described for the northern sectors of the Mediterranean at times coincident with the so-called North Atlantic “Heinrich Events” of massive ice-rafting (Rohling et al., 1998b; Paterne et al., 1999; Cacho et al., 1999, 2000, 2001, 2002).

Within the last glacial cycle, periods of intensified or more frequent northerly cooling events in the Mediterranean generally correlate with the so-called Dansgaard-Oeschger (DO) stadials (cold episodes), and the most intense events correlate with the most intense DO stadials, which were marked in the North Atlantic by the Heinrich Events. Highly resolved records from the Mediterranean region furthermore indicate that the cool periods were characterised by enhanced aridity (e.g., Allen et al., 1999; Sanchez-Goñi et al., 2002; Combourieu-Nebout et al., 2002; Tzedakis et al., 2004; Hoogakker et al., 2004).

The most recent sapropel (S1) formed between about 9,000 and 6,000 calibrated years BP, in association with the monsoon maximum of the current interglacial period. Detailed work has found an “interruption” in the deposition of the S1 sapropel, marking a period of improved deepwater ventilation that spans several centuries around 8,500-8,000 years BP (Van Straaten, 1966, 1970, 1972, 1985; Rohling et al., 1997; De Rijk et al., 1999; Geraga et al., 2000; Mercone et al., 2000, 2001; Casford et al., 2001, 2002, 2003; Rohling et al., 2002a). This ventilation event coincided with intensified cooling over the Adriatic and Aegean Seas, which has been related to an increase in the intensity or frequency of northerly cold outbursts over those regions, in association with a widespread North Atlantic cold event (Rohling et al., 2002a). Similarly, the ending of sapropel deposition was marked by a cooling, around 6,000 years BP (Rohling et al., 1997; Geraga et al., 2000; Casford et al., 2001, 2002, 2003; Mercone et al., 2001; Rohling et al., 2002a). Pollen data confirms that the cooling periods were normally marked by enhanced aridity (e.g., Rossignol-Strick, 1995; Geraga et al., 2000). Episodically improved deepwater ventilation within times of generally poor ventilation (sapropel conditions) has since been inferred for a large number of sapropels, suggesting that climatic variability on short time-scales persisted even in these periods of generally warm and humid conditions in the Mediterranean region (Casford et al., 2003).

The above might give the impression that sapropels resulted from monsoon maxima extending over several millennia, while some internal variability occurred due to intermittent cooling events originating from the north, in association with polar or temperate climate events. This would be misleading, because the centennial-scale episodes of increased cooling from the north are well known to have been associated with severe reductions in monsoon runoff. One likely example is the 800-year monsoon interruption within Eemian sapropel S5 (e.g., Cane et al., 2000; Rohling et al., 2002b; 2004). Monsoon-fed African lakes show a similar “interruption” within the Holocene monsoon maximum, as part of a series of distinct and abrupt periods of low lake-levels that coincide in time with the northerly coolings recorded in the

Mediterranean, as described above. The particularly pronounced period of low lake levels between 8.5 and 7.8 ka BP (Gasse, 2000) coincides closely with the “interruption” of sapropel S1, and recent compilations have found this to be a widespread interval of climate deterioration throughout (at least) the Northern Hemisphere (Mayewski et al., 2004; Rohling and Pälike, 2005). Furthermore, Egyptian archaeological records for the Holocene indicate dramatic turnovers related to strong fluctuations in intensity and frequency of Nile flooding (Hassan, 1997, 2002 (edited volume), and references therein). Clearly, some fundamental, if elusive, connection exists between cooling from the north and reductions in (African) monsoon intensity. Hence, it is worthwhile to spend some time looking at variability in the wind-blown dust flux into the Mediterranean, as a measure of North African climate variability.

At present, the northward transport of aeolian (wind-blown) dust over the Mediterranean is linked to the presence of cyclones over the basin (Moulin et al., 1997), and most Saharan dust deposition over southern Europe occurs with precipitation (Bücher and Lucas, 1984; Bergametti et al., 1989a; Loyer-Pilot et al., 1989; Guerzoni et al., 1992). Important source areas of dust transport to Western Europe are Algeria, the Western Sahara and the Moroccan Atlas (Molinaroli, 1996; Avila et al., 1997; Goudie and Middleton, 2001; Chapter 19). Weldeab et al. (2002) use Si/Al and Ti/Al ratios as well as Sr and Nd isotopes to show that the Saharan terrigenous input into the western Mediterranean Sea is predominantly from the southwest (Morocco/ northwestern Algeria) and southeast (Tunisia/ western Libya) during interglacial periods and from the southern Saharan/Sahelian region during glacial times. Eastern Libya and Egypt are the important source areas of aeolian dust to the eastern Mediterranean basin. Overall, terrigenous input into the Mediterranean at glacial times greatly exceeded that of interglacial times (Weldeab et al., 2002). Fluvial sediment yields were also higher (Macklin et al., 2002).

A continuous 3 million-year record of dust supply from the northern Sahara into the eastern Mediterranean, developed from sediment magnetic data, consistently shows dust-flux minima at times of northern hemisphere insolation/monsoon maxima (Larrasoña et al., 2003). These minima were related to northward penetration of the African summer monsoon front beyond the central Saharan watershed (~21°N), as proposed previously on the basis of Mediterranean oxygen isotope data (Rohling et al., 2002b). Such northward penetration of the African summer monsoon agrees with a broad expansion of (savannah-like) vegetation cover in both observations and modelling experiments (“greening of the Sahara”: Claussen et al., 1998; Brovkin et al., 1998; Irizarry-Ortiz et al., 2003; and references therein). Consequently increased soil cohesiveness throughout large areas of the northern Sahara would cause a decrease in dust production, similar to modern conditions in the Sahel (Middleton, 1985).

A high-resolution record of lithogenic fraction variability from the Alboran Sea has revealed millennial- to submillennial-scale oscillations. These correlate with Atlantic Dansgaard-Oeschger stadials and Heinrich Events, and were characterised by increases in the northward Saharan dust transport (Moreno et al., 2002). Similar increases in Saharan dust supply at times of DO stadials have been inferred from sediment cores throughout the wider western Mediterranean (Hoogakker et al., 2004), and detailed magnetic susceptibility records for cores taken in the eastern

Mediterranean (pp. 3/28-3/31 in Hemleben et al., 2003) suggest that a millennial-scale aeolian dust signal may also be preserved in that basin.

At this stage, we do not infer that the monsoon penetration model inferred for the longer-term (Milankovitch-scale) dust cycles should apply to the shorter-term (sub-Milankovitch) events. Instead, the shorter-term dust-flux variations may well be controlled by cyclone activity, as it appears to be on interannual to decadal time scales (Moulin et al., 1997). An important control on cyclogenesis within the Mediterranean basin is exerted by cold (arid) air outbursts over the northern sectors, and this may be the mechanism underlying the correlation between dust cycles in the Mediterranean and DO events in the North Atlantic region. This interpretation remains speculative, however, until more process-oriented research leads to a more detailed understanding.

Figure Captions.

Figure 1. Map of the Mediterranean Sea.

Figure 2. Longitudinal cross-section showing water mass circulation in the Mediterranean Sea during the present-day winter (after Wüst, 1961). Isolines indicate salinity values in p.s.u. and arrows indicate the direction of water circulation in the Mediterranean Sea.

Figure 3. Surface water circulation in the Mediterranean Sea (after Vergnaud-Grazzini et al., 1988; Roussenov et al., 1995). Shaded areas indicate intermediate and deep water formation.

Figure 4. Northern Hemisphere summer atmospheric circulation pattern. The main winds are indicated as arrows. ITCZ = Inter-Tropical Convergence Zone, H = areas of high sea-level pressure, L = areas of low sea-level pressure (modified after Rossignol-Strick, 1985, Reichart, 1997).

Figure 5. Schematic illustration of surface circulation in the Alboran Sea (modified after Tintoré et al., 1988).

Figure 6. Schematic illustration of the main gyres associated with Atlantic surface flow. IAS = Ionian-Atlantic Stream, CC = Cilician Current, AMC = Asia Minor Current, MMJ = Mid-Mediterranean Jet (from Robinson et al., 1992).

Figure 7. Typical salinity profiles for the western (dots) and eastern (squares) Mediterranean basins (after Rohling and Bryden, 1992).

Figure 8. Schematic illustration of the preconditioning phase, and the violent mixing and deep convection phase. E = Evaporation (modified after Rohling et al., 1998).

Fig. 9 – salinities Estimated sea surface salinity distribution for (A) the Holocene Climate Optimum and (B) the Last Glacial Maximum (after Myers et al., 1998), based on surface-water d¹⁸O distribution patterns (de Rijk et al., 1999a,b).

Figure 10. Annual sea surface temperature (SST) reconstructions for the HCO and LGM based on the artificial neural network (ANN) technique. To avoid any impacts of the 8.2 ka BP cold event, we defined the Holocene Climatic Optimum (HCO) as the interval between 8.3 ka BP and 9.5 ka BP. A total of 42 cores was selected for this time slice. In contrast, 37 cores were used for the Last Glacial Maximum (LGM) between 19 and 23 ka BP. The SST estimates for each core were obtained by calculating the average SSTs from all the samples within the defined time slices, based on a calibration of >300 core-top samples.

Figure 11. Schematic presentation of the changes in subsurface circulation patterns between the present day and times of sapropel formation. The three profiles presented summarise information obtained from analytical and modelling studies from North to South through the Adriatic and Aegean basins, and from West (Strait of Sicily) to East (near Cyprus) through the open eastern Mediterranean. MIW stands for Mediterranean Intermediate Water; ADW for Adriatic Deep water; AeDW for Aegean Deep water; AIW for Adriatic Intermediate Water; AeIW for Aegean intermediate Water; ODW for Old (isolated) Deep Water. Modified after Rohling (1994) and Myers et al. (1998).

Figure 12. Phase relationships between the sapropel record and associated δ¹⁸O record from core RC9-181 and the orbital cycles of precession and eccentricity (modified after Hilgen, 1991).

Plate 1. Scanning electron microscope images of the carbonate shells of several planktonic foraminiferal species that live in the Mediterranean Sea. **1, 2** *Globigerina bulloides* d'Orbigny; **1** umbilical view and **2** spiral view. **3, 4** *Globoturborotalita rubescens* Hofker; **3** umbilical view and **4** spiral view. **5, 6** *Turborotalita quinqueloba* (Natland); **5** umbilical view and **6** spiral view. **7, 8** *Globigerinoides ruber* (d'Orbigny). **9, 10** *Globigerinoides sacculifer* (Brady); **9** umbilical view and **10** spiral view. **11, 12** *Globigerinella digitata* (Brady); **11** umbilical view and **12** spiral view. **13-15** *Globigerinella siphonifera* (d'Orbigny); **13** umbilical view, **14** peripheral view, and **15** spiral view. Each scale bar represents 100 μm.

Plate 2. Example of a laminated sapropel in a freshly opened sediment core. The thick dark bed recovered over two core sections represents sapropel S5 from the previous interglacial maximum, 124-119 thousand years ago. The core was recovered during cruise M53-1 of *R. V. Meteor* in November-December 2001 (chief scientist Prof. Ch. Hemleben).

References Rohling et al.

- Adamson, D. A., Gasse, F., Street, F. A. and Williams, M. A. J. (1980), Late Quaternary history of the Nile, *Nature*, 288: 50-55.
- Allen, J. R., Brandt, U., Brauer, A., Hubberten, H. W., Huntley, B., Keller, J., Kraml, M., Mackensen, A., Mingram, J., Negendank, J. F. W., Nowaczyk, N. R., Oberhansli, H., Watts, W. A., Wulf, S., and Zolitschka, B. (1999), Rapid environmental changes in southern Europe during the last glacial period, *Nature*, 400: 740-743.
- Arnone, R. A., Wiesenburg, D. A., and Saunders, K. (1990), The origin and characteristics of the Algerian current, *Journal of Geophysical Research*, 95: 1587-1598.
- Arz, H. W., Lamy, F., Pätzold, J., Müller, P. J., and Prins, M. (2003), Mediterranean moisture source for an early-Holocene humid period in the Northern Red Sea, *Science*, 300: 118-121.
- Avila, A., Queralt-Mitjans, L., and Alarcón, M. (1997), Mineralogical composition of African dust delivered by red rains over northeastern Spain, *Journal of Geophysical Research*, 102: 21977-21996.
- Bard, E., Delaygue, G., Rostek, F., Antonioli, F., Silenzi, S., and Schrag, D. P. (2002), Hydrological conditions over the western Mediterranean basin during the deposition of the cold Sapropel 6 (ca. 175 kyr BP), *Earth and Planetary Science Letters*, 202: 481-494.
- Bar-Matthews, M., Ayalon, A., Gilmour, M., Matthews, A., and Hawkssworth, C. (2003), Sea-land oxygen isotopic relationships from planktonic foraminifera and speleothems in the Eastern Mediterranean region and their implication for paleorainfall during interglacial intervals, *Geochimica et Cosmochimica Acta*, 67: 3181-3199.
- Bar-Matthews, M., Ayalon, A., Kaufman, A. (2000), Timing and hydrological conditions of Sapropel events in the Eastern Mediterranean, as evident from speleothems, Soreq cave, Israel, *Chemical Geology*, 169: 145-156
- Bar-Matthews, M., Ayalon, A., Kaufman, A., and Wasserburg, G. J. (1999), The Eastern Mediterranean paleoclimate as a reflection of regional events: Soreq cave, Israel, *Earth and Planetary Science Letters*, 166: 85-95.
- Bergametti, G., Dutot, L., Buat-Ménard, P., and Remoudaki, E. (1989), Seasonal variability of the elemental composition of atmospheric aerosol particles over the northwestern Mediterranean, *Tellus*, 41B: 553-561.
- Béthoux, J. P. (1984), Paleo-hydrologie de la Mer Méditerranée au cours des derniers 20 000 ans, *Oceanologica Acta*, 7: 43-48.
- Béthoux, J. P. and Gentili, B. (1994), The Mediterranean Sea, a test area for marine and climatic interactions, in P. Malanotte-Rizzoli and A. R. Robinson (eds.), *Ocean Processes in Climate Dynamics: Global and Mediterranean Examples* (Kluwer Academic Publishers, Neth.) 239-254.
- Béthoux, J. P., Gentili, B., Morin, P., Nicolas, E., Pierre, C. and Ruiz-Pino, D. (1999) The Mediterranean Sea: a miniature ocean for climatic and environmental studies and a key for the climatic functioning of the North Atlantic, *Progress in Oceanography*, 44: 131-146.
- Boucher, K. (1975) *Global climate* (The English University Press Ltd., London) 326 pp.
- Broecker, W. S. (2000), Abrupt climate change: causal constraints provided by the paleoclimate record, *Earth Science Reviews*, 51: 137-154.
- Brovkin, V., Claussen, M., Petoukhov, V., and Ganopolski, A. (1998), On the stability of the atmosphere-vegetation system in the Sahara/Sahel region, *Journal of Geophysical Research*, 103: 31613-31624
- Bruce, J.G., and Charnock, H. (1965), Studies of winter sinking of cold water in the Aegean Sea, *Rapports Com. Internat. Mer Méditerranée*, 18: 773-778.
- Bryden, H. L., and Kinder, T.H. (1991), Steady two-layer exchange through the Strait of Gibraltar, *Deep-Sea Research*, 38: S445-S463.
- Bryden, H. L., Candela, J., and Kinder, T. H. (1994), Exchange through the Strait of Gibraltar, *Progress in Oceanography*, 33: 201-248.
- Bücher, A., and Lucas, G. (1984), Sédimentation éolienne intercontinentale, poussières sahariennes et géologie, *Bull. Centr. Rech. Expl.-Prod. Elf-Aquit.* 8: 151-165.
- Burman, I., and Oren, O. H. (1970), Water outflow close to the bottom from the Aegean, *Cahiers Océanographique*, 22: 775-780.
- Cacho, I., Grimalt, J. O., and Canals, M. (2002), Response of the Western Mediterranean Sea to rapid climatic variability during the last 50,000 years: a molecular biomarker approach, *Journal of Marine Systems*, 33- 34: 253-272.
- Cacho, I., Grimalt, J. O., Canals, M., Sbaffi, L., Shackleton, N. J., Schönfeld, J., and Zahn, R. (2001), Variability of the western Mediterranean Sea surface temperatures during the last 25,000 years and its connection with the northern hemisphere climatic changes, *Paleoceanography*, 16: 40-52.

- Cacho, I., Grimalt, J. O., Pelejero, C., Canals, M., Sierro, F. J., Flores, J. A., and Shackleton, N. J. (1999), Dansgaard-Oeschger and Heinrich event imprints in Alboran Sea paleotemperatures. *Paleoceanography* 14: 698-705.
- Cacho, I., Grimalt, J. O., Sierro, F. J., Shackleton, N. J., and Canals, M. (2000), Evidence of enhanced Mediterranean thermohaline circulation during rapid climate coolings, *Earth and Planetary Science Letters*, 183: 417-429.
- Cane, T., Rohling, E. J., Kemp, A. E. S., Cooke, S., and Pearce, R. B. (2002), High-resolution stratigraphic framework for Mediterranean sapropel S5: defining temporal relationships between records of Eemian climate variability, *Palaeogeography, Palaeoclimatology, Palaeoecology*, 183: 87-101.
- Cantu, V. (1977), The climate of Italy, in: C.C Wallen (ed.), *Climates of Central and Southern Europe - World survey of climatology*, 6 (Elsevier , Amsterdam) 127-183.
- Casford, J. S. L., Abu-Zied, R. H., Rohling, E. J., Cooke, S., Boessenkool, K. P., Brinkhuis, H., de Vries, C., Wefer, G., Geraga, M., Papatheodorou, G., Croudace, I., Thomson, J., Wells, N. C., and Lykousis, V. (2001), Mediterranean climate variability during the Holocene, *Mediterranean Marine Science*, 2: 45-55
- Casford, J. S. L., Rohling, E. J., Abu-Zied, R. H., Cooke, S., Fontanier, C., Leng, M., and Lykousis, V. (2002), Circulation changes and nutrient concentrations in the Late Quaternary Aegean Sea: A non-steady state concept for sapropel formation, *Paleoceanography* , 17, doi 10.1029/2000PA000601.
- Casford, J. S. L., Rohling, E. J., Abu-Zied, R. H., Jorissen, F. J., Leng, M., and Thomson, J. (2003), A dynamic concept for eastern Mediterranean circulation and oxygenation during sapropel formation, *Palaeogeography, Palaeoclimatology, Palaeoecology*, 190: 103-119.
- Castradori, D. (1993), Calcareous nannofossils and the origin of eastern Mediterranean sapropels, *Paleoceanography*, 8: 459-471.
- Cheney, R. E., and Doblar, R. A. (1982), Structure and variability of the Alboran Sea frontal system, *Journal of Geophysical Research*, 87: 585-594.
- Cita, M.B., and Grignani, D. (1982), Nature and Origin of Late Neogene Mediterranean Sapropels, in S. O. Schlanger and M. B. Cita (eds.) *Nature and Origin of Cretaceous Carbon-Rich Facies* (Academic, San Diego, California) 165-196.
- Cita, M.B. (1973), Inventory of biostratigraphical findings and problems, in W.B.F. Ryan, K.J. Hsü et al. (eds.), *Initial Reports of the Deep-Sea Drilling Project*, 13 (U.S. Govt. Printing Office, Washington, D.C.) 1045-1073.
- Cita, M. B., Vergnaud-Grazzini, C., Robert, C., Chamley, H., Ciarranfi, N., and d'Onofrio, S. (1977), Paleoclimatic record of a long deep sea core from the eastern Mediterranean, *Quaternary Research*, 8: 205-235.
- Claussen, M., Browkin, V., Ganopolski, A., Kubatski, C., and Petoukhov, V. (1998), Modelling global terrestrial vegetation-climate interaction. *Philosophical Transactions Royal Society, London*, 353: 53-63.
- Clemens, S. C., and Prell, W. L. (1990), Late Pleistocene variability of Arabian Sea summer monsoon winds and continental aridity: eolian records from the lithogenic component of deep-sea sediments, *Paleoceanography*, 5: 109-145.
- Clemens, S. C., Murray, D. W., and Prell, W. L. (1996), Nonstationary phase of the Plio-Pleistocene Asian monsoon, *Science*, 274: 943-948.
- COHMAP members (1988), Climatic changes of the last 18,000 years: observations and model simulations, *Science*, 241: 1043-1052.
- Combourieu-Nebout, N., Turon, J. L., Zahn, R., Capotondi, L., Londeix, L., and Pahnke, K. (2002), Enhanced aridity and atmospheric high-pressure stability over the western Mediterranean during the North Atlantic cold events of the past 50 k.y., *Geology*, 30: 863-866.
- Corselli, C., Principato, M. S., Maffioli, P., and Crudelli, D. (2002), Changes in planktonic assemblages during sapropel S5 deposition: Evidence from Urania Basin area, eastern Mediterranean, *Paleoceanography*, 17: doi 10.1029/2000PA000536.
- Cramp, A., and O'Sullivan, G. (1999), Neogene sapropels in the Mediterranean: a review. *Marine Geology*, 153: 11-28.
- Dansgaard, W., Johnsen, S. J., Clausen, H. B., Dahl-Jensen, D., Gundestrup, N. S., Hammer, C. U., Hvidberg, C. S., Steffensen, J. P., Sveinbjornsdottir, A. E., Jouzel, J., and Bond, G. (1993), Evidence for general instability of past climate from a 250 kyr ice core, *Nature*, 364: 218-219.
- De Rijk, S., Rohling, E. J., and Hayes, A. (1999), Onset of climatic deterioration in the eastern Mediterranean around 7 ky BP; micropalaeontological data from Mediterranean sapropel interruptions, *Marine Geology*, 153: 337-343.

- Digerfeldt, G., Olsson, S., and Sandgren, P. (2000), Reconstruction of lake-level changes in lake Xinias, central Greece, during the last 40,000 years, *Palaeogeography, Palaeoclimatology, Palaeoecology*, 158: 65-82.
- Dinarès-Turell, J., Hoogakker, B. A. A., Roberts, A. P., Rohling, E. J., and Sagnotti, L. (2003), Quaternary climatic control of biogenic magnetite production and eolian dust input in cores from the Mediterranean Sea, *Palaeogeography, Palaeoclimatology, Palaeoecology*, 190: 195-209.
- Dünkeloh, A., and Jacobbeit, J. (2003), Circulation dynamics of Mediterranean precipitation variability 1948-1998, *International Journal of Climatology*, 23: 1843-1866.
- El Dardir, M. (1994), Sedimentation in the Nile High Dam reservoir, 1987-1992, and sedimentary futurologic aspects, *Sedimentology of Egypt*, 2: 23-39.
- Elenga, H., Peyron, O., Bonneville, R., Jolly, D., Cheddadi, R., Guiot, J., Andrieu, V., Bottema, S., Bucher, G., de Beaulieu, J. L., Hamilton, A. C., Maley, J., Marchant, R., Perez-Obiol, R., Reille, M., Riollet, G., Scott, L., Straka, H., Taylor, D., Van Campo, E., Vincens, A., Laarif, F., and Jonson, H. (2000), Pollen-based biome reconstruction for southern Europe and Africa, 18,000 yr BP, *Journal of Biogeography*, 27: 621-634.
- Emeis, K. C., Camerlenghi, A., McKenzie, J. A., Rio, D., and Sprovieri, R. (1991), The occurrence and significance of Pleistocene and Upper Pliocene sapropels in the Tyrrhenian Sea, *Marine Geology*, 100: 155-182.
- Emeis, K. C., Schulz, H., Struck, U., Rossignol-Strick, M., Erlenkeuser, H., Howell, M. W., Kroon, D., Mackensen, H., Ishizuka, S., Oba, T., Sakamoto, T., and Koizumi, I. (2003), Eastern Mediterranean surface water temperatures and $\delta^{18}\text{O}$ composition during deposition of sapropels in the late Quaternary, *Paleoceanography*, 18: doi1029/2000PA000617.
- Emeis, K. C., Schulz, H. M., Struck, U., Sakamoto, T., Doose, H., Erlenkeuser, H., Howell, M., Kroon, D., and Paterne, M. (1998), Stable isotope and temperature records of sapropels from ODP Sites 964 and 967: Constraining the physical environment of sapropel formation in the Eastern Mediterranean Sea, in: A. H. F. Robertson, K. C. Emeis, C. Richter, and A. Camerlenghi (eds.), *Proceedings ODP, Scientific Results*, 160 (Ocean Drilling Program, College Station, TX) 309-331.
- Emeis, K. C., Struck, U., Schulz, H. M., Bernasconi, S., Sakamoto, T., and Martinez-Ruiz, F. (2000), Temperature and salinity of Mediterranean Sea surface waters over the last 16,000 years: Constraints on the physical environment of S1 sapropel formation based on stable oxygen isotopes and alkenone unsaturation ratios, *Palaeogeography, Palaeoclimatology, Palaeoecology*, 158: 259-280.
- Fairbanks, R. G. (1989), A 17,000 year glacio-eustatic sea level record: influence of glacial melting rates on the Younger Dryas event and deep-ocean circulation, *Nature*, 342: 637-642.
- Fairbanks, R. G. (1990), The age and origin of the "Younger Dryas Climate Event" in Greenland Ice Cores, *Paleoceanography*, 5: 937-948.
- Foucault, A., and Mélières, F. (2000), Palaeoclimatic cyclicity in central Mediterranean Pliocene sediments: the mineralogical signal, *Palaeogeography, Palaeoclimatology, Palaeoecology*, 158: 311-323.
- Frogley, M. R., Tzedakis, P. C., and Heaton, T. H. E. (1999), Climate variability in Northwest Greece during the last interglacial, *Science*, 285: 1886-1889.
- Ganssen, G., and Troelstra, S. R. (1987), Palaeoenvironmental changes from stable isotopes in planktonic foraminifera from Eastern Mediterranean Sapropels, *Marine Geology*, 75: 221-230.
- Garrett, C. (1994), The Mediterranean Sea as a climate test basin, in P. Malanotte-Rizzoli and A.R. Robinson (eds.), *Ocean Processes in Climate Dynamics: Global and Mediterranean Examples* (Kluwer Academic Publishers, Neth.) 227-237.
- Garzoli, S., and Maillard, C. (1979), Winter circulation in the Sicily and Sardinia straits region, *Deep-Sea Research*, 26A: 933-954.
- Gascard, J. C. (1978), Mediterranean deep water formation, baroclinic instability and oceanic eddies, *Oceanologica Acta*, 1: 315-330.
- Gascard, J. C., and Richez, C. (1985), Water mass and circulation in the western Alboran Sea and in the Strait of Gibraltar, *Progress in Oceanography*, 15: 157-216.
- Gasse, F. (2000), Hydrological changes in the African tropics since the last glacial maximum, *Quaternary Science Reviews*, 19: 189-211.
- Gaven, C., Hillaire-Marcel, C., and Petit-Maire, N. (1981), A Pleistocene lacustrine episode in southeastern Libya, *Nature*, 290: 131-133.
- Geraga, M., Tsaila-Monopolis, S., Ioakim, Chr., Papatheodorou, G., and Ferentinos, G. (2000), Evaluation of palaeoenvironmental changes during the last 18,000 years in the Myrtoon basin, SW Aegean Sea, *Paleogeography, Palaeoclimatology, Palaeoecology*, 156: 1-17.

- Gilman, C., and Garrett, C. (1994), Heat flux parameterizations for the Mediterranean Sea: The role of atmospheric aerosols and constraints from the water budget, *Journal of Geophysical Research*, 99: 5119-5134.
- Goudie, A.S., and Middleton, N.J. (2001), Saharan dust storms: nature and consequences, *Earth Science Reviews*, 56: 179-204
- Grootes, P. M., Stuiver, M., White, J. W. C., Johnsen, S., and Jouzel, J. (1993), Comparison of oxygen isotope records from the GISP2 and GRIP Greenland ice cores, *Nature*, 366: 552-554.
- Guerzoni, S., Landuzzi, W., Lenaz, R., Quarantotto, G., Cesari, G., Rampazzo, R., and Molinaroli, E., (1992), Mineral atmospheric particulate from south to northwest Mediterranean: seasonal variations and characteristics, *Water Pollution Research Reports*, 28: 483-493.
- Hassan, F. A. (1997), The dynamics of a riverine civilization: a geoarchaeological perspective on the Nile Valley, Egypt, *World Archaeology*, 29: 51-74.
- Hassan, F. A. (2002) (ed.), *Droughts, Food, and culture: ecological change and food security in Africa's later prehistory* (Kluwer Academic/ Plenum Publishers, New York).
- Hayes, A., Kucera, M., Kallel, N., Sbaffi, L., and Rohling, E. J. (2005), Glacial Mediterranean sea surface temperatures reconstructed from planktonic foraminiferal assemblages, *Quaternary Science Reviews*, 24: 999-1016.
- Heburn, G. W., and La Violette, P. E. (1990), Variations in the structure of the anticyclonic gyres found in the Alboran Sea, *Journal of Geophysical Research*, 92: 2901-2906.
- Hemleben, Ch., Hoernle, K., Jørgensen, B. B., and Roether, W. (2003), *Ostatlantik-Mittelmeer-Schwarzes Meer, Cruise 51, 12 September-28 December 2001, Meteor Berichte*, 03-1, 213 pp.
- Hemming, S. R. (2004), Heinrich events: Massive detritus layers of the North Atlantic and their global climate impact, *Reviews in Geophysics*, 42: RG1005, doi10.1029/2003RG 000128.
- Higgs, N. C., Thomson, J., Wilson, T. R. S., and Croudace, I. W. (1994), Modification and complete removal of eastern Mediterranean sapropels by postdepositional oxidation, *Geology*, 22: 423-426.
- Hilgen, F. J. (1991a), Astronomical calibration of Gauss to Matuyama sapropels in the Mediterranean and implication for the geomagnetic Polarity Time Scale, *Earth and Planetary Science Letters*, 104: 226-244.
- Hilgen, F.J. (1991b), Extension of the astronomically calibrated(polarity) timescale to the Miocene/ Pliocene boundary, *Earth and Planetary Science Letters*, 107: 349-368.
- Hilgen, F. J., Krijgsman, W., Langereis, C. G., Lourens, L. J., Santarelli, A., and Zachariasse, W. J. (1995), Extending the astronomical (polarity) time scale into the Miocene. *Earth and Planetary Science Letters*, 136: 495-510.
- Hilgen, F. J., Lourens, L. J., Berger, A., and Loutre, M. F. (1993), Evaluation of the astronomically calibrated time scale for the late Pliocene and earliest Pleistocene, *Paleoceanography*, 8: 549-656.
- Hill, A. E. & Mitchelson-Jacob, E. G. (1993), Observations of a poleward-flowingsaline core on the continental slope west of Scotland, *Deep-Sea Research*, 40, 1521-1527.
- Hoelzmann, P., Kruse, H. J., and Rottinger, F. (2000), Precipitation estimates for the eastern Saharan palaeomonsoon based on a water balance model of the West Nubian Palaeolake Basin, *Global and Planetary Change*, 26: 105-120.
- Hoogakker, B.A.A., Rothwell, R.G., Rohling, E.J., Paterne, M., Stow, D.A.V., Herrle, J.O., and Clayton, T. (2004) Aridity episodes during the last glacial cycle recorded in calcium carbonate records from the western Mediterranean Sea, *Marine Geology*, 211: 21-43.
- Hurst, H. E. (1944), *A short account of the Nile Basin. Physical Department, Ministry of Public Works, Egypt, Paper 45*, 77pp.
- Imbrie, J., Boyle, E. A., Clemens, S. C., Duffy, A., Howard, W. R., Kukla, G., Kutzbach, J., Martinson, D. G., McIntyre, A., Mix, A. C., Molino, B., Morley, J. J., Peterson, L. C., Pisias, N. G., Prell, W. L., Raymo, M. E., Shackleton, N. J., and Toggweiler, J. R. (1992), On the structure and origin of major glaciation cycles. 1. Linear responses to Milankovitch forcing, *Paleoceanography*, 7: 701-738.
- Imbrie, J., Shackleton, N. J., Pisias, N. G., Morley, J. J., Prell, W. L., Martinson, D. G., Hays, J. D., McIntyre, A., and Mix, A. C. (1984), The orbital theory of Pleistocene climate: support from a revised chronology of the marine $\delta^{18}\text{O}$ record, in A. Berger, J. Imbrie, J. Hays, G. Kukla, and B. Saltzman (eds.), *Milankovitch and Climate: understanding the response to astronomical forcing* (D.Reidel, Hingham, Massachusetts, USA) 269-305.
- Iorga, M. C., and Lozier, M. S. (1999), Signatures of the Mediterranean outflow from a North Atlantic climatology 1. Salinity and density fields, *Journal of Geophysical Research*, 104, 25985-26009.
- Irizarry-Ortiz, M. M., Wang, G., and Eltahir, E. A. B. (2003), Role of the biosphere in the mid-Holocene climate of West Africa, *Journal of Geophysical Research*, 108: doi10.1029/2001JD000989.
- Jenkins, J. A., and Williams, D. F. (1984), Nile water as a cause of eastern Mediterranean sapropel formation: evidence for and against, *Marine Micropaleontology*, 9: 521-534.

- Jongsma, D., Fortuin, A. R., Huson, W., Troelstra, S. R., Klaver, G. T., Peters, J. M., Van Harten, D., De Lange, G. J., and Ten Haven, L. (1983), Discovery of an anoxic basin within the Strabo Trench, eastern Mediterranean, *Nature*, 305: 795-797.
- Jorissen, F. J. (1999), Benthic foraminiferal successions across Late Quaternary Mediterranean sapropels. *Marine Geology*, 153: 91-101.
- Jorissen, F. J., Asioli, A., Borsetti, A. M., Capotondi, L., De Visscher, J. P., Hilgen, F. J., Rohling, E. J., Van der Borg, K., Vergnaud-Grazzini, C., and Zachariasse, W. J. (1993), Late Quaternary central Mediterranean biochronology, *Marine Micropaleontology*, 21: 169-189.
- Kallel, N., Paterne, M., Duplessy, J. C., Vergnaud-Grazzini, C., Pujol, C., Labeyrie, L., Arnold, M., Fontugne, M., and Pierre, C. (1997a), Enhanced rainfall in the Mediterranean region during the last sapropel event, *Oceanologica Acta*, 20: 697-712.
- Kallel, N., Paterne, M., Labeyrie, L., Duplessy, J. C., Arnold, M. (1997b), Temperature and salinity records of the Tyrrhenian Sea during the last 18,000 years, *Palaeogeography, Palaeoclimatology, Palaeoecology*, 135: 97-108.
- Kemp, A. E. S., Pearce, R. B., Koizumi, I., Pike, J., and Rance, S. J. (1999), The role of mat-forming diatoms in the formation of Mediterranean sapropels, *Nature*, 398: 57-61.
- Klein, B., Roether, W., Manca, B. B., Bregant, D., Beitzel, V., Kovacevic, V., and Luchetta, A. (1999), The large deep water transient in the eastern Mediterranean, *Deep-Sea Research*, 46: 371-414.
- Krom, M. D., Cliff, R. A., Eijsink, L. M., Herut, B., and Chester, R. (1999), The characterisation of Saharan dust and Nile particulate matter in surface sediments from the Levantine basin using Sr isotopes, *Marine Geology*, 155: 319-330.
- Kullenberg, B. (1952), On the salinity of the water contained in marine sediments, *Medd. Oceanogr. Inst. Göteborg*, 21: 1-38.
- Kutzbach, J. E. (1985), Modeling of paleoclimates, in Issues in atmospheric and oceanic modeling, A; climate dynamics, in S. Manabe (ed.) *Advances in Geophysics*, 28: 161-196.
- Kutzbach, J. E., and Guetter, P. J. (1986), The influence of changing orbital parameters and surface boundary conditions on climate simulations for the past 18,000 years, *Journal of Atmospheric Science*, 43: 1726-1759.
- Langway Jr., C. C., Oeschger, H., and Dansgaard, W. (1985) (eds.), Greenland Ice Core: Geophysics, geochemistry, and the environment. *Geophysical Monograph*, 33 (American Geophysical Union, Washington DC), 118pp.
- Larrasoña, J., Roberts, A. P., Rohling, E. J., Winklhofer, M., and Wehausen, R. (2003), Three million years of monsoon variability over the northern Sahara, *Climate Dynamics*, 21: 689-698.
- Lascaratos, A. (1989), Hydrology of the Aegean Sea. *Reports in Meteorology and Oceanography*, 40 (vol I.): 313-431.
- Laskar, J. (1999), The limits of Earth orbital calculations for geological time scale use. *Philosophical Transactions Royal Society, London A*, 357: 1735-1759.
- Laskar, J., Joutel, F., and Boudin, F. (1993), Orbital precessional, and insolation quantities for the Earth from -20 to +10 Myr, *Astronomy and Astrophysics*, 270: 522-533.
- La Violette, P. E. (1986), Short term measurements of surface currents associated with the Alboran Sea during ?Donde Va?., *Journal of Physical Oceanography*, 16: 262-279.
- Leaman, K. D., and Schott, F. A. (1991), Hydrographic structure of the convection regime in the Gulf of Lions: Winter 1987, *Journal of Physical Oceanography*, 21: 575-598.
- Lolis, C. J., Bartzokas, A., and Katsoulis, B. D. (2002), Spatial and temporal 850 hPa air temperature and sea-surface temperature covariances in the Mediterranean region and their connection to atmospheric circulation, *International Journal of Climatology*, 22: 663-676.
- Lourens, L. J., Antonarakou, A., Hilgen, F. J., Van Hoof, A. A. M., Vergnaud-Grazzini, C., and Zachariasse, W. J. (1996), Evaluation of the Plio-Pleistocene astronomical time-scale, *Paleoceanography*, 11: 391-413.
- Lourens, L. J., Hilgen, F. J., Gudjonsson, L., and Zachariasse, W. J. (1992), Late Pliocene to early Pleistocene astronomically forced sea surface productivity and temperature variations in the Mediterranean, *Marine Micropaleontology*, 19: 49-78.
- Lourens, L. J., Wehausen, R., and Brumsack, H. J. (2001), Geological constraints on tidal dissipation and dynamical ellipticity of the earth over the past three million years. *Nature*, 409: 1029-1033.
- Loye-Pilot, M-D., Martin, J. M., and Morelli, J. (1989), Atmospheric input of particulate matter and inorganic nitrogen to the northwestern Mediterranean, *Water Pollution Research Reports*, 13: 368-376.
- Macklin, M. G., Fuller, I. C., Lewin, J., Maas, G. S., Passmore, D. G., Rose, J., Woodward, J. C., Black, S., Hamlin, R. H. B., and Rowan, J. S. (2002), Correlation of fluvial sequences in the Mediterranean

- basin over the last 200 ka and their relationship to climate change, *Quaternary Science Reviews*, 21: 1633-1641.
- Magri, D., and Parra, I. (2002), Late Quaternary western Mediterranean pollen records and African wind, *Earth and Planetary Science Letters*, 200: 401-408.
- Maheras, P., Xoplaki, E., Davies, T., Martin-Vide, J., Bariendos, M., and Alcoforado, M. J. (1999), Warm and cold monthly anomalies across the Mediterranean basin and their relationship with circulation; 1860-1990, *International Journal of Climatology*, 19: 1697-1715.
- Malanotte-Rizzoli, P., and Bergamasco, A. (1989), The circulation of the eastern Mediterranean. Part I, *Oceanologica Acta*, 12: 335-351.
- Malanotte-Rizzoli, P., and Bergamasco, A. (1991), The wind and thermally driven circulation of the eastern Mediterranean Sea. Part II: the baroclinic case, *Dynamics Atmosphere Oceans*, 15: 355-419.
- Malanotte-Rizzoli, P., and Hecht, A. (1988), Large-scale properties of the eastern Mediterranean: a review, *Oceanologica Acta*, 11: 323-335.
- Mandel, R. D., and Simmons, A. H. (2001), Prehistoric Occupation of Late Quaternary Landscapes near Kharga Oasis, Western Desert of Egypt, *Geoarchaeology*, 16: 95-117.
- Martinson, D. G., Pisias, N. G., Hayes, J. D., Imbrie, J., Moore, T. C., and Shackleton, N. J. (1987), Age dating and the orbital theory of the ice-ages: development of a high-resolution 0 to 300,000 year chronostratigraphy, *Quaternary Research*, 27: 1-29.
- Matthews A., Ayalon A., and Bar-Matthews M. (2000), D/H ratios of fluid inclusions of Soreq Cave (Israel) speleothems as a guide to the Eastern Mediterranean Meteoric Line relationships in the last 120 ky, *Chemical Geology*, 166: 183-191.
- Matthiessen, S., and Haines, K. (2003), A hydraulic box model study of the Mediterranean response to postglacial sea-level rise, *Paleoceanography*, 18: doi1029/2003PA000880.
- Mayewski, P.A., Rohling, E.J., Stager, J.C., Karlén, W., Maasch, K., Meeker, L.D., Meyerson, E., Gasse, F., Van Kreveld, S., Holmgren, K., Lee-Thorp, J., Rosqvist, G., Rack, F., Staubwasser, M., Schneider, R.R., Steig, E. (2004), Holocene Climate Variability, *Quaternary Research*, 62: 243-255.
- McGill, D. A. (1961), A preliminary study of the oxygen and phosphate distribution in the Mediterranean Sea, *Deep-Sea Research*, 8: 259-269.
- McKenzie, J.A. (1993), Pluvial conditions in the eastern Sahara following the penultimate deglaciation: implications for changes in atmospheric circulation patterns with global warming, *Palaeogeography, Palaeoclimatology, Palaeoecology*, 103: 95-105.
- MEDATLAS (1997), *Mediterranean Hydrographic Atlas* (Mast Supporting Initiative; MAS2-CT93-0074): CD-ROM.
- MEDOC group (1970), Observation of formation of deep water in the Mediterranean Sea, *Nature*, 277: 1037-1040.
- MEDRIFF consortium (1995), Three brine lakes discovered in the seafloor of the eastern Mediterranean, *EOS*, 76: pp. 313 & 318.
- Mercone, D., Thomson, J., Abu-Zied, R. H., Croudace, I. W., and Rohling, E. J. (2001), High-resolution geochemical and micropalaeontological profiling of the most recent eastern Mediterranean sapropel, *Marine Geology*, 177: 25-44.
- Mercone, D., Thomson, J., Croudace, I. W., Siani, G., Paterne, M., Troelstra, S. (2000), Duration of S1, the most recent sapropel in the eastern Mediterranean Sea, as indicated by accelerator mass spectrometry radiocarbon and geochemical evidence, *Paleoceanography*, 15: 336-347.
- Meyers, P. A., and Negri, A. (2003) (eds.), Paleoclimatic and Paleoceanographic Records in Mediterranean Sapropels and Mesozoic Black Shales, *Palaeogeography, Palaeoclimatology, Palaeoecology*, 190: 480 pp.
- Middleton, N. J. (1985), Effect of drought on dust production in the Sahel, *Nature*, 409: 431-434.
- Miller, A. R. (1963), Physical Oceanography of the Mediterranean Sea: A discourse. *Rapp. Comm. Int. Mer Médit.*, 17: 857-871.
- Miller, A. R. (1972), Speculations concerning bottom circulation in the Mediterranean Sea, in D. J. Stanley (ed.), *The Mediterranean Sea* (Dowden, Hutchinson and Ross, Stroudsburg, Pa.) 37-42.
- Miller, A. R. (1974), Deep convection in the Aegean Sea, *Coll. Int. CNRS*, 215: 155-163.
- Miller, A. R., Tchernia, P., Charnock, H., and McGill, D.A. (1970), *Mediterranean Sea Atlas of Temperature, Salinity, Oxygen: Profiles and Data From Cruises of R.V. Atlantis and R.V. Chain, With Distribution of Nutrient Chemical Properties*, A. E. Maxwell et al. (eds.) (Alpine, Braintree, Mass.) 190 pp.
- Molinaroli, E. (1996), Mineralogical characterisation of Saharan dust with a view to its final destination in Mediterranean sediments, in S. Guerzone and R. Chester (eds.), *The impact of desert dust across the Mediterranean* (Kluwer Academic Publishing) 153-162.

- Mommersteeg, H. J. P. M., Loutre, M. F., Young, R., Wijmstra, T. A., and Hooghiemstra, H. (1995), Orbital forced frequencies in the 975,000 year pollen record from Tenaghi Philippon (Greece), *Climate Dynamics*, 11: 4-24.
- Moreno, A., Cacho, I., Canals, M., Prins, M. A., Sánchez-Goñi, M. F., Grimalt, J. O., and Weltje, G. J. (2002), Saharan dust transport and high-latitude glacial climatic variability: the Alboran Sea record, *Quaternary Research*, 58: 318-328.
- Moses, T., Kiladis, G. N., Diaz, H. F., and Barry, R. G. (1987), Characteristics and frequency of reversals in mean sea level pressure in the North Atlantic sector and their relationship to long-term temperature trends, *Journal of Climatology*, 7: 13-30.
- Moulin, C., Lambert, C.E., Dulac, F., and Dayan, U. (1997), Control of atmospheric export of dust from North Africa by the North Atlantic Oscillation, *Nature*, 387: 691-694.
- Myers, P.G. (2002), Flux-forced simulations of the paleocirculation of the Mediterranean, *Paleoceanography*, 17: doi 10.1029/2000PA000613.
- Myers, P. G., Haines, K., and Rohling, E. J. (1998), Modelling the paleo-circulation of the Mediterranean: The last glacial maximum and the Holocene with emphasis on the formation of sapropel S1, *Paleoceanography*, 13: 586-606.
- Naval Oceanography Command (1987), *U.S. Navy climatic study of the Mediterranean Sea* (Naval Oceanography Command Detachment, Asheville, North Carolina) 342 pp.
- Nijenhuis, I. A., Schenau, S. J., Van der Weijden, C. H., Hilgen, F. J., Lourens, L. J., and Zachariasse, W. J. (1996), On the origin of upper Miocene sapropelites: a case study from the Faneromeni section, Crete (Greece), *Paleoceanography*, 11: 633-645.
- Nof, D. (1979), On man-induced variations in the circulation of the Mediterranean Sea, *Tellus*, 31: 558-564.
- Nolet, G. J., and Corliss, B. H. (1990), Benthic foraminiferal evidence for reduced deep-water circulation during sapropel formation in the eastern Mediterranean, *Marine Geology*, 94: 109-130.
- Olausson, E. (1961), Studies of deep-sea cores, *Reportsof the Swedish Deep Sea Expedition 1947-1948*, 8: 353-391.
- O'Neill-Baringer, M., and Price, J. F. (1999), A review of the physical oceanography of the Mediterranean outflow, *Marine Geology*, 155, 63-82.
- Ozsoy, E. (1981), On the atmospheric factors affecting the Levantine Sea. *European Centre for Medium Range Weather Forecasts, Technical Report*, 25: 29 pp.
- Pachur, H. J. (2001), Holozäne Klimawechsel in den nördlichen Subtropen, *Nova Acta Leopoldina NF88*, 331: 109-131.
- Pachur, H. J., and Braun, G. (1980), The paleoclimate of the central Sahara, Libya and the Libyan Desert, *Palaeoecology of Africa*, 12: 351-363.
- Pälike, H., and Shackleton, N. J. (2000), Constraints on astronomical parameters from the geological record for the last 25 Myr, *Earth and Planetary Science Letters*, 182: 1-14.
- Parrilla, G., Kinder, T. H. and Preller, R. H. (1986), Deep and intermediate Mediterranean water in the western Alboran Sea, *Deep-Sea Research*, 33: 55-88.
- Paterne, M., Kallel, N., Labeyrie, L., Vautravers, M., Duplessy, J. C., Rossignol-Strick, M., Cortijo, E., Arnold, M., and Fontugne, M. (1999), Hydrological relationship between the North Atlantic ocean and the Mediterranean during the past 15-75 kyr, *Paleoceanography*, 14: 626-638.
- Peltier, W. R. (2004), Global glacial isostacy and the surface of the ice-age earth: the ICE-5G (VM2) model and GRACE, *Annual Review Earth and Planetary Science*, 32, 111-149.
- Perissoratis, C., and Piper, D. J. W. (1992), Age, regional variation and shallowest occurrence of S₁ sapropel in the northern Aegean Sea, *Geomarine Letters*, 12: 49-53.
- Perkins, H. and Pistek, P. (1990), Circulation in the Algerian Basin during June 1986, *Journal of Geophysical Research*, 95: 1577-1585.
- Petit-Maire, N., and Guo, Z. (1997), In-phase Holocene climate variations in the present-day desert areas of China and Northern Africa, in J. Meco and N. Petit-Maire, *Climates of the Past, Proceedings of the UNESCO-IUGS, June 2-7, 1995, CLIP meeting* (Universidad de Las Palmas, Gran Canaria, Spain) 137-140.
- Pinardi, N., and Masetti, E. (2000), Variability of the large scale general circulation of the Mediterranean Sea from observations and modelling: a review, *Palaeogeography, Palaeoclimatology, Palaeoecology*, 158: 153-173.
- Pisias, N. G., and Moore, T. C. (1981), The evolution of Pleistocene climate: a time series approach, *Earth and Planetary Science Letters*, 52: 450-458.
- Pistek, P., De Strobel, F. and Montanari, C. (1985), Deep Sea circulation in the Alboran Sea, *Journal of Geophysical Research*, 90: 4969-4976.

- POEM group (1992), General circulation of the eastern Mediterranean Sea, *Earth-Science Reviews*, 32: 285-308.
- Pollak, M. I. (1951), The sources of deep water of the eastern Mediterranean Sea, *Deep-Sea Research*, 10: 128-152.
- Poulos, S. E., Drakopoulos, P. G., and Collins M. B. (1997), Seasonal variability in sea surface oceanographic conditions in the Aegean Sea (eastern Mediterranean): an overview, *Journal of Marine Systems*, 13: 225-244.
- Prell, W. L. (1984), Covariance patterns of foraminiferal $\delta^{18}\text{O}$: and evaluation of Pliocene ice volume changes near 3.2. million years ago, *Science*, 226: 692-694.
- Prell, W. L., and Kutzbach, J. E. (1987), Monsoon variability over the past 150,000 years, *Journal of Geophysical Research*, 92: 8411-8425.
- Prentice, I. C., Guiot, J., Harrison, S. P. (1992), Mediterranean vegetation, lake levels and palaeoclimate at the last glacial maximum, *Nature*, 360: 658-660.
- Price, J. F., O'Neil Baringer, M., Lueck, R. G., Johnson, G. C., Ambar, I., Parilla, G., Cantos, A., Kennelly, M. A., and Sanford, T. B. (1993), Mediterranean outflow mixing and dynamics, *Science*, 259: 1277-1282.
- Reid, J. L. (1979), On the contribution of the Mediterranean Sea outflow to the Norwegian-Greenland Sea, *Deep-Sea Research*, 26A, 1199-1223.
- Reichart, G.J. (1997), Late Quaternary variability of the Arabian Sea monsoon and oxygen minimum zone, *Geologica Ultraiectina*, 154, pp. 174.
- Reiss, Z., Halicz, E., and Luz, B. (1999). Late-Holocene foraminifera from the SE Levantine Basin, *Israel Journal of Earth Science*, 48: 1-27.
- Richardson, P. L., Bower, A. S. and Zenk, W. (2000), A census of meddies tracked by floats, *Progress in Oceanography*, 45: 209-250, 2000.
- Richardson, P. L., McCartney, M. S., and Maillard. C. (1991), A search for meddies in historical data. *Dynamics of Atmospheres and Oceans*, 15: 241-265.
- Richez, C. and Gascard, J. C. (1986), Mediterranean water flows when approaching the Strait of Gibraltar, *Deep-Sea Research*: 135-137.
- Ritchie, J. C., Eyles, C. H., and Haynes, C. V. (1985), Sediment and pollen evidence for an early to mid-Holocene humid period in the eastern Sahara, *Nature*, 314: 352-355.
- Robinson, A.R. and Golnaraghi, M. (1994), The physical and dynamical oceanography of the Mediterranean Sea, in P. Malanotte-Rizzoli and A. R. Robinson (eds.), *Ocean Processes in Climate Dynamics: Global and Mediterranean Examples* (Kluwer Academic Publishers, Neth.) 255-306.
- Robinson, A.R. et al. (1992), General circulation of the eastern Mediterranean, *Earth Science Reviews*, 32: 285-309.
- Rodwell, M. J., and Hoskins, B. J. (1996), Monsoons and the dynamics of deserts, *Quarterly Journal of the Royal Meteorological Society*, 122: 1385-1404.
- Roether, W. and Schlitzer, R. (1991), Eastern Mediterranean deep water renewal on the basis of chlorofluoromethane and tritium data, *Dynamics Atmosphere and Oceans*, 15: 333-354.
- Roether, W., and Well, R. (2001), Oxygen consumption in the Eastern Mediterranean, *Deep-Sea Research I*, 48: 1535-1551, 2001.
- Roether, W., Manca, B. B., Klien, B., Bregant, D., Georgopoulos, D., Beitzel, V., Kovacevic, V. and Luchetta, A. (1996), Recent changes in Eastern Mediterranean Deep Waters, *Science*, 271: 333-335.
- Roether, W., Schlosser, P., Kuntz, R. and Weiss, W. (1983), Transient tracer studies of the thermohaline circulation of the Mediterranean, *Manuscripts for Mediterranean circulation, NATO Workshop*, 44 p.
- Rognon, P. (1987), Aridification and abrupt climatic events on the Saharan northern and southern margins, 20,000 years BP to present, in W. H. Berger and L. D. Labeyrie (eds.), *Abrupt Climatic Change: Evidence and Implications* (D. Reidel Publishing Company, Dordrecht) 209-220.
- Rohling, E. J. (1991a), A simple two-layered model for shoaling of the eastern Mediterranean pycnocline due to glacio-eustatic sea level lowering, *Paleoceanography*, 6: 537-541.
- Rohling, E. J. (1991b), Shoaling of the eastern Mediterranean pycnocline due to reduction of excess evaporation: implications for sapropel formation, *Paleoceanography*, 6: 747-753.
- Rohling, E. J. (1994), Review and new aspects concerning the formation of Mediterranean sapropels, *Marine Geology*, 122: 1-28.
- Rohling, E. J. (1997), Mutual influencing between the Atlantic Ocean and the Mediterranean Sea during the Quaternary, in: J. Meco and N. Petit-Maire, *Proceedings of the IUGS-UNESCO CLIP IV meeting, Canary Islands* (Universidad de Las Palmas, Gran Canaria, Spain) 141-149.
- Rohling, E. J. (1999a), Environmental controls on salinity and $\delta^{18}\text{O}$ in the Mediterranean, *Paleoceanography*, 14: 706-715.

- Rohling, E. J. (1999b) (ed.), Mediterranean paleoclimate and sapropel studies, *Marine Geology*, 153: 350 pp.
- Rohling, E. J., and Bryden, H. L. (1992), Man-induced salinity and temperature increases in western Mediterranean Deep Water, *Journal of Geophysical Research*, 97: 11191-11198.
- Rohling, E. J., and Bryden, H. L. (1994), Estimating past changes in the eastern Mediterranean freshwater budget, using reconstructions of sea level and hydrography. *Proceedings Koninklijke Nederlandse Akademie, Ser.B.*, 97: 201-217.
- Rohling, E. J., and De Rijk, S. (1999a), The Holocene Climate Optimum and Last Glacial Maximum in the Mediterranean: the marine oxygen isotope record, *Marine Geology*, 153: 57-75.
- Rohling, E. J., and De Rijk, S. (1999b), Erratum to "The Holocene Climate Optimum and Last Glacial Maximum in the Mediterranean: the marine oxygen isotope record," *Marine Geology*, 161: 385-387.
- Rohling, E. J., and Gieskes, W. W. C. (1989), Late Quaternary changes in Mediterranean Intermediate Water density and formation rate, *Paleoceanography*, 4: 531-545.
- Rohling, E. J., and Hilgen, F. J. (1991), The eastern Mediterranean climate at times of sapropel formation: a review, *Geologie en Mijnbouw*, 70: 253-264.
- Rohling, E. J. and Pälike, H. (2005), Centennial-scale climate deterioration with a superimposed cold event around 8,200 years ago, *Nature*, 434, 975-979, 2005.
- Rohling, E. J., and Zachariasse, W. J. (1996), Red Sea outflow during the Last Glacial Maximum, *Quaternary International*, 31: 77-83.
- Rohling, E. J., Cane, T. R., Cooke, S., Sprovieri, M., Bouloubassi, I., Emeis, K. C., Schiebel, R., Kroon, D., Jorissen, F. J., Lorre, A., and Kemp, A. E. S. (2002b), African monsoon variability during the previous interglacial maximum, *Earth and Planetary Science Letters*, 202: 61-75.
- Rohling, E. J., Den Dulk, M., Pujol, C. and Vergnaud-Grazzini, C. (1995), Abrupt hydrographic change in the Alboran Sea (western Mediterranean) around 8000 yrs BP, *Deep-Sea Research*, 42: 1609-1619.
- Rohling, E. J., Fenton, M., Jorissen, F. J., Bertrand, P., Ganssen, G., and Caulet, J. P. (1998a), Magnitudes of sea-level lowstands of the past 500,000 years, *Nature*, 394:162-165.
- Rohling, E. J., Hayes, A., De Rijk, S., Kroon, D., Zachariasse, W. J. and Eisma, D. (1998b), Abrupt cold spells in the northwest Mediterranean, *Paleoceanography*, 13: 316-322.
- Rohling, E. J., Jorissen, F. J., and De Stigter, H. C. (1997), 200 Year interruption of Holocene sapropel formation in the Adriatic Sea, *Journal of Micropalaeontology*, 16: 97-108.
- Rohling, E. J., Jorissen, F. J., Vergnaud-Grazzini, C., and Zachariasse, W. J. (1993a), Northern Levantine and Adriatic planktonic foraminifera: reconstruction of paleoenvironmental gradients, *Marine Micropaleontology*, 21: 191-218.
- Rohling, E. J., Mayewski, P. A., and Challenor, P. (2003), On the timing and mechanism of millennial-scale climate variability during the last glacial cycle, *Climate Dynamics*, 20: 257-267.
- Rohling, E. J., Mayewski, P. A., Hayes, A., Abu-Zied, R. H., and Casford, J. S. L. (2002a), Holocene atmosphere-ocean interactions: records from Greenland and the Aegean Sea, *Climate Dynamics*, 18: 587-593.
- Rohling, E. J., Sprovieri, M., Cane, T. R., Casford, J. S. L., Cooke, S., Bouloubassi, I., Emeis, K. C., Schiebel, R., Rogerson, M., Hayes, A., Jorissen, F. J., and Kroon, D. (2004), Reconstructing past planktic foraminiferal habitats using stable isotope data: a case history for Mediterranean sapropel S5, *Marine Micropaleontology*, 50: 89-123.
- Rohling, E. J., Vergnaud-Grazzini, C., and Zaalberg, R. (1993b), Temporary repopulation by low-oxygen tolerant benthic foraminifera within an Upper Pliocene sapropel: Evidence for the role of oxygen depletion in the formation of sapropels, *Marine Micropaleontology*, 22: 207-219.
- Rose, J., Meng, X., Watson, C. (1999), Palaeoclimate and palaeoenvironment responses in the western Mediterranean over the last 140,000 ka: evidence from Mallorca, Spain, *Journal of the Geological Society*, 156: 435-448.
- Rossignol-Strick, M. (1983), African monsoons, an immediate climate response to orbital insolation, *Nature*, 30: 446-449.
- Rossignol-Strick, M. (1985), Mediterranean Quaternary sapropels, an immediate response of the African monsoon to variations of insolation, *Palaeogeography, Palaeoclimatology, Palaeoecology*, 49: 237-263.
- Rossignol-Strick, M. (1987), Rainy periods and bottom water stagnation initiating brine accumulation and metal concentrations: 1. the Late Quaternary, *Paleoceanography*, 2: 333-360.
- Rossignol-Strick, M. (1995), Sea-land correlation of pollen records in the eastern Mediterranean for the glacial-interglacial transition: biostratigraphy versus radiometric time-scale, *Quaternary Science Reviews*, 14: 893-915.

- Rossignol-Strick, M., Nesteroff, V., Olive, P., and Vergnaud-Grazzini, C. (1982), After the deluge; Mediterranean stagnation and sapropel formation, *Nature*, 295: 105-110.
- Roussenov, V., Stanev, E., Artale, V., and Pinardi, N. (1995), A seasonal model of the Mediterranean Sea general circulation, *Journal of Geophysical Research*, 100: 13515-13538.
- Ruddiman, W. F., and Kutzbach, J. E. (1989), Forcing of Late Cenozoic northern hemisphere climate by plateau uplift in southern Asia and the American West, *Journal of Geophysical Research*, 94: 18409-18427.
- Ruddiman, W. F., McIntyre, A., and Raymo, M. (1987), Paleoenvironmental results from North Atlantic sites 607 and 609, in: W. F. Ruddiman et al., *Initial Reports Deep Sea Drilling Project*, 94: 855-878.
- Ruddiman, W. F., Raymo, M., Martinson, D., Clement, B., and Backman, J. (1989), Pleistocene evolution: northern hemisphere ice sheets and North Atlantic Ocean, *Paleoceanography*, 4: 353-412.
- Ruddiman, W. F., Raymo, M., and McIntyre, A. (1986), Matuyama 41,000-year cycles: North Atlantic Ocean and northern hemisphere ice sheets, *Earth and Planetary Science Letters*, 80: 117-129.
- Rumney, G. R. (1968), *Climatology and the World's climates* (Macmillan Company, New York) 656pp.
- Saaroni, H., Bitan, A., Alpert, P., and Ziv, B. (1996), Continental Polar outbreaks into the Levant and Eastern Mediterranean, *International Journal of Climatology*, 16: 1175-1191.
- Said, R. (1981), *The geological evolution of the River Nile* (Springer-Verlag, New York) 151 pp.
- Samuel, S., Haines, K., Josey, S., and Myers, P. G. (1999), Response of the Mediterranean Sea thermohaline circulation to observed changes in the winter wind stress field in the period 1980-1993, *Journal of Geophysical Research*, 104: 7771-7784.
- Sanchez-Goñi, M. F., Sierro, F. J., Peypouquet, J. P., Grimalt, J. O., Shackleton, N. J., Cacho, I., Turon, J. L., and Guiot, J. (2002), Synchronicity between marine and terrestrial responses to millennial scale climatic variability during the last glacial period in the Mediterranean region, *Climate Dynamics*, 19: 95-105.
- Schlitzer, R., Roether, W., Oster, H., Junghans, H. G., Hausmann, M., Johannsen, H., and Michelato, A. (1991), Chlorofluoromethane and oxygen in the eastern Mediterranean, *Deep-Sea Research*, 38: 1531-1551.
- Schmiedl, G., Mitschele, A., Beck, S., Emeis, K. C., Hemleben, Ch., Schultz, H., Sperling, M., and Weldeab, S. (2003), Benthic foraminiferal record of ecosystem variability in the eastern Mediterranean Sea during times of sapropel S₅ and S₆ deposition, *Palaeogeography, Palaeoclimatology, Palaeoecology*, 190: 139-164.
- Scientific Staff Cruise BAN84 (1985), Gypsum precipitation from cold brines in an anoxic basin in the eastern Mediterranean, *Nature*, 314: 152-154.
- Scrivner, A., Vance, D., and Rohling, E. J. (2004), New neodymium isotope data quantify Nile involvement in Mediterranean anoxic episodes, *Geology*, 32: 565-568.
- Shackleton, N. J., and Opdyke, N. D. (1973), Oxygen isotope and paleomagnetic stratigraphy of equatorial Pacific core V28-238: Oxygen isotope temperatures and ice volume on a 10⁵ and 10⁶ year time scale, *Quaternary Research*, 3: 39-55.
- Shackleton, N. J., and Opdyke, N. D. (1976), Oxygen isotope and paleomagnetic stratigraphy of equatorial Pacific core V28-238, late Pliocene to latest Pleistocene, in: R. M. Cline and J. D. Hays (eds.), *Investigations of Late Quaternary Palaeoceanography and Palaeoclimatology, Memoirs of the Geological Society of America*, 145: 449-464.
- Shackleton, N. J., and Opdyke, N. D. (1977), Oxygen isotope and paleomagnetic evidence for early northern hemisphere glaciation, *Nature*, 270: 216-219.
- Sharaf, El Din (1977), Effect of Aswan High Dam on the Nile flood and on the estuarine and coastal circulation pattern along the Mediterranean Egyptian coast, *Limnology and Oceanography*, 22: 194-207.
- Shaw, H. F., and Evans, G. (1984), The nature, distribution and origin of a sapropelic layer in sediments of the Cilicia Basin, northeastern Mediterranean, *Marine Geology*, 61: 1-12.
- Shimmield, G. B., Mowbray, S. R., and Weedon, G. P. (1990), A 350-ka history of the Indian Southwest monsoon – evidence from deep-sea cores, northwest Arabian Sea, *Transactions of the Royal Society, Edinburgh, Earth Science*, 81: 289-299.
- Siddall, M., Rohling, E. J., Almogi-Labin, A., Hemleben, Ch., Meischner, D., Schmelzer, I., and Smeed, D. A. (2003), Sea-level fluctuations during the last glacial cycle, *Nature*, 423: 853-858.
- Stanley, D. J. (1978), Ionian Sea sapropel distribution and late Quaternary palaeoceanography in the eastern Mediterranean, *Nature*, 274: 149-152.
- Stanley, D. J. (1996), Nile Delta: extreme case of sediment entrapment on a delta plain and consequent coastal land loss, *Marine Geology*, 129: 189-195.
- Stanley, D. J. and Wingerath, J. (1996), Clay mineral distributions to interpret Nile cell provenance and dispersal: I. Lower River Nile to delta, *Journal of Coastal Research*, 12: 911-929.

- Stanley, D. J., Nir, Y., and Galili, E. (1998), Clay mineral distributions to interpret Nile cell provenance and dispersal: II. Offshore margin between Nile to delta and northern Israel, *Journal of Coastal Research*, 14: 196-217.
- Stommel, H., Bryden, H., and Mangelsdorf, P. (1973), Does some of the Mediterranean outflow come from great depth? *Pure and Applied Geophysics*, 105: 879-889.
- Stratford, K., Williams, R. G., and Myers, P. G. (2000), Impact of the circulation on sapropel formation in the eastern Mediterranean, *Global Biogeochemical Cycles*, 14: 683-695.
- Suc, J. P. (1984), Origin and evolution of the Mediterranean vegetation and climate in Europe, *Nature*, 307: 429-432.
- Szabo, B. J., Haynes, C. V. Jr., and Maxwell, T. A. (1995), Ages of Quaternary pluvial episodes determined by uranium-series and radiocarbon dating of lacustrine deposits of Eastern Sahara, *Palaeogeography, Palaeoclimatology, Palaeoecology*, 113: 227-242.
- Tang, C. M., and Stott, L. D. (1993), Seasonal salinity changes during Mediterranean sapropel deposition 9000 years B.P.: evidence from isotopic analyses of individual planktonic foraminifera, *Paleoceanography*, 8: 473-493.
- Theocharis, A., (1989), Deep water formation and circulation in the Aegean Sea, *Reports in Meteorology and Oceanography*, 40(I): 335-359.
- Theocharis, A., and Georgopoulos, D. (1993), Dense water formation over the Samothraki and Limnos Plateaux in the north Aegean Sea (eastern Mediterranean Sea), *Continental Shelf Research*, 13: 919-939.
- Thomson, J., Higgs, N. C., Wilson, T. R. S., Croudace, I. W., De Lange, G. J., and Van Santvoort, P. J. M. (1995), Redistribution and geochemical behaviour of redox-sensitive elements around S1, the most recent eastern Mediterranean sapropel, *Geochimica et Cosmochimica Acta*, 59: 3487-3501.
- Thomson, J., Mercone, D., de Lange, G. J., and van Santvoort, P. J. M. (1999), Review of recent advances in the interpretation of eastern Mediterranean sapropel S1 from geochemical evidence, *Marine Geology*, 153: 77-89.
- Thunell, R. C. (1986), Pliocene-Pleistocene climatic changes: evidence from land-based and deep-sea marine records, *Mem. Societa Geologica Italiana*, 31: 135-143.
- Thunell, R. C., and Williams, D. F. (1983), Paleotemperature and paleosalinity history of the eastern Mediterranean during the late Quaternary, *Palaeogeography, Palaeoclimatology, Palaeoecology*, 44: 23-39.
- Thunell, R. C., and Williams, D. F. (1989), Glacial-Holocene salinity changes in the Mediterranean Sea: hydrographic and depositional effects, *Nature*, 338: 493-496.
- Thunell, R.C., Williams, D. F., and Cita, M. B. (1983), Glacial anoxia in the eastern Mediterranean, *Journal of Foraminiferal Research*, 13: 283-290.
- Thunell, R. C., Williams, D. F. and Howell, M. (1987), Atlantic-Mediterranean water exchange during the late Neogene, *Paleoceanography*, 2: 661-678.
- Thunell, R. C., Williams, D. F., and Kennett, J. P. (1977), Late Quaternary paleoclimatology, stratigraphy and sapropel history in eastern Mediterranean deep-sea sediments, *Marine Micropaleontology*, 2: 371-388.
- Thunell, R. C., Rio, D., Sprovieri, R., and Vergnaud-Grazzini, C. (1991), An overview of the post-Messinian paleoenvironmental history of the western Mediterranean, *Paleoceanography*, 6: 143-164.
- Tintoré, J. D., La Violette, P. E., Blade, I., and Cruzado, A. (1988), A study of an intense density front in the eastern Alboran Sea: The Almeria-Oran Front, *Journal of Physical Oceanography*, 18: 1384-1397.
- Trewartha, G. T. (1966), *The earth's problem climates* (Methuen & Co., London) 334 pp.
- Trigo, I. F., Davies, T. D., and Bigg, G. R. (1999), Objective climatology in the Mediterranean region, *Journal of Climate*, 12: 1685-1696.
- Trigo, I. F., Davies, T. D., and Bigg, G. R. (2000), Decline in Mediterranean rainfall caused by weakening of Mediterranean cyclones, *Geophysical Research Letters*, 27: 2913-2916.
- Troelstra, S. R. (1987), Late Quaternary sedimentation in Tyro and Kretheus Basins, southeast of Crete, *Marine Geology*, 75: 77-91.
- Tzedakis, P. C. (1993), Long-term tree populations in northwest Greece through multiple climatic cycles, *Nature*, 364: 437-440.
- Tzedakis, P. C. (1999), The last climatic cycle at Kopais, central Greece, *Journal of the Geological Society, London*, 156: 425-434.
- Tzedakis, P. C., Frogley, M. R., Lawson, I. T., Preece, R. C., Cacho, I., and de Abreu, L. (2004), Ecological thresholds and patterns of millennial-scale climate variability: the response of vegetation in Greece during the last glacial period, *Geology*, 32: 109-112.

- UNDP/UNESCO (1978), *Coastal protection studies. Project Findings and Recommendations* (Paris: UNDP/EGY/73/063) 483 pp.
- Van Os, B. J. H., Lourens, L. J., Hilgen, F. J., De Lange, G. J., and Beaufort, L. (1994), The formation of Pliocene sapropels and carbonate cycles in the Mediterranean: diagenesis, dilution, and productivity, *Paleoceanography*, 9: 601-617.
- Van Straaten, L. M. J. U. (1966), Micro-Malacological investigation of cores from the southeastern Adriatic Sea, *Proceedings Koninklijke Nederlandse Akademie Sciences, Serie B*, 69: 429-445.
- Van Straaten, L. M. J. U. (1970), Holocene and late-Pleistocene sedimentation in the Adriatic Sea, *Geologische Rundschau*, 60: 106-131.
- Van Straaten, L. M. J. U. (1972), Holocene stages of oxygen depletion in deep waters of the Adriatic Sea, in D. J. Stanley (ed.), *The Mediterranean Sea* (Dowden, Hutchinson & Ross Inc., Stroudsburg, Pa.) 631-643.
- Van Straaten, L. M. J. U. (1985), Molluscs and sedimentation in the Adriatic Sea during late-Pleistocene and Holocene times, *Giornale Geologia, Serie 3a*, 47: 181-202.
- Vergnaud-Grazzini, C. (1985), Mediterranean late Cenozoic stable isotope record: stratigraphic and paleoclimatic implications, in D. J. Stanley and F. C. Wezel (eds.), *Geological evolution of the Mediterranean Basin* (Springer-Verlag, New York) 413-451.
- Vergnaud-Grazzini, C., Borsetti, A. M., Cati, F., Colantoni, P., d'Onofrio, S., Saliège, J. F., Sartori, R., and Tampieri, R. (1988), Palaeoceanographic record of the last deglaciation in the Strait of Sicily, *Marine Micropaleontology*, 13: 1-21.
- Vergnaud-Grazzini, C., Capotondi, L., and Lourens, L. J. (1993), A refined Pliocene to early Pleistocene chronostratigraphic frame at ODP Hole 653A (West Mediterranean), *Marine Geology*, 117: 329-349.
- Vergnaud-Grazzini, C., Ryan, W. B. F., and Cita, M. B. (1977), Stable isotope fractionation, climatic change and episodic stagnation in the eastern Mediterranean during the late Quaternary, *Marine Micropaleontology*, 2, 353-370: 1977.
- Verhallen, P. J. J. M. (1991), Late Pliocene to Early Pleistocene Mediterranean mud-dwelling foraminifera; influence of a changing environment on community structure and evolution. *Utrecht Micropaleontological Bulletin*, 40: 219 pp.
- Voelker, A. H., et al. (2002), Global distribution of centennial-scale records for marine isotope stage (MIS) 3: a database, *Quaternary Science Reviews*, 21: 1185-1212.
- Wahby, S. D., and Bishara, N. F. (1981), The effect of the river Nile on Mediterranean water, before and after the construction of the High Dam at Aswan, in J. M. Martin, J. D. Burton, and D. Eisma (eds.), *River inputs to Ocean Systems* (UNEP-UNESCO, Switzerland) 311-318.
- Wallmann, K., Suess, E., Westbrook, G. H., Winkler, G., Cita, M. B., and the MEDRIFF consortium (1997), Salty brines on the Mediterranean sea floor, *Nature*, 387: 31-32.
- Wehausen, R., and Brumsack H. J. (2000), Chemical cycles in Pliocene sapropel-bearing and sapropel-barren eastern Mediterranean sediments, *Palaeogeography, Palaeoclimatology, Palaeoecology*, 158: 325-352.
- Weldeab, S., Emeis, K.C., Hemleben, C., Siebel, W. (2002), Provenance of lithogenic surface sediments and pathways of riverine suspended matter in the Eastern Mediterranean Sea: evidence from $^{143}\text{Nd}/^{144}\text{Nd}$ and $^{87}\text{Sr}/^{86}\text{Sr}$ ratios, *Chemical Geology*, 186: 139-149.
- Wijmstra, T. A., Young, R., and Witte, H. J. L. (1990), An evaluation of the climatic conditions during the Late Quaternary in northern Greece by means of multivariate analysis of palynological data and comparison with recent phytosociological and climatic data, *Geologie en Mijnbouw*, 69: 243-251.
- Williams, D. F., Thunell, R. C., and Kennett, J. P. (1978), Periodic fresh-water flooding and stagnation of the eastern Mediterranean during the late Quaternary, *Science*, 201: 252-254.
- Williams, M. A. J., Adamson, D. A., Cock, B., and McEvedy, R. (2000), Late Quaternary environments in the White Nile region, Sudan, *Global and Planetary Change*, 26: 305-316.
- Wüst, G. (1960), Die tiefenzirkulation des Mitteläandischen Meeres in den Kernschichten des Zwischen- und des Tiefenwassers, *Deutsche Hydrographische Zeitschrift*, 13: 105-131.
- Wüst, G. (1961), On the vertical circulation of the Mediterranean Sea, *Journal of Geophysical Research*, 66: 3261-3271.
- Yüce, H. (1995), Northern Aegean water masses, *Estuarine, Coastal and Shelf Science*, 41: 325-343.
- Zachariasse, W. J., and Spaak, P. (1983), Middle Miocene to Pliocene paleoenvironmental reconstruction of the Mediterranean and adjacent Atlantic Ocean: planktonic foraminiferal record of southern Italy, in J. E. Meulenkamp (ed.), *Reconstruction of marine paleoenvironments*, *Utrecht Micropaleontological Bulletin*, 30: 91-110.
- Zachariasse, W. J., Gudjonsson, L., Hilgen, F. J., Langereis, C. G., Lourens, L. J., Verhallen, P. J. J. M., and Zijderveld, J. D. A. (1990), Late Gauss to Early Matuyama invasions of *Neogloboquadrina*

atlantica in the Mediterranean and associated record of climatic change, *Paleoceanography*, 5: 239-252.

Zachariasse, W. J., Zijderveld, J. D. A., Langereis, C. G., Hilgen, F. J., and Verhallen, P. J. J. M. (1989), Early Late Pliocene biochronology and surface water temperature variations in the Mediterranean, *Marine Micropaleontology*, 14: 339-355.

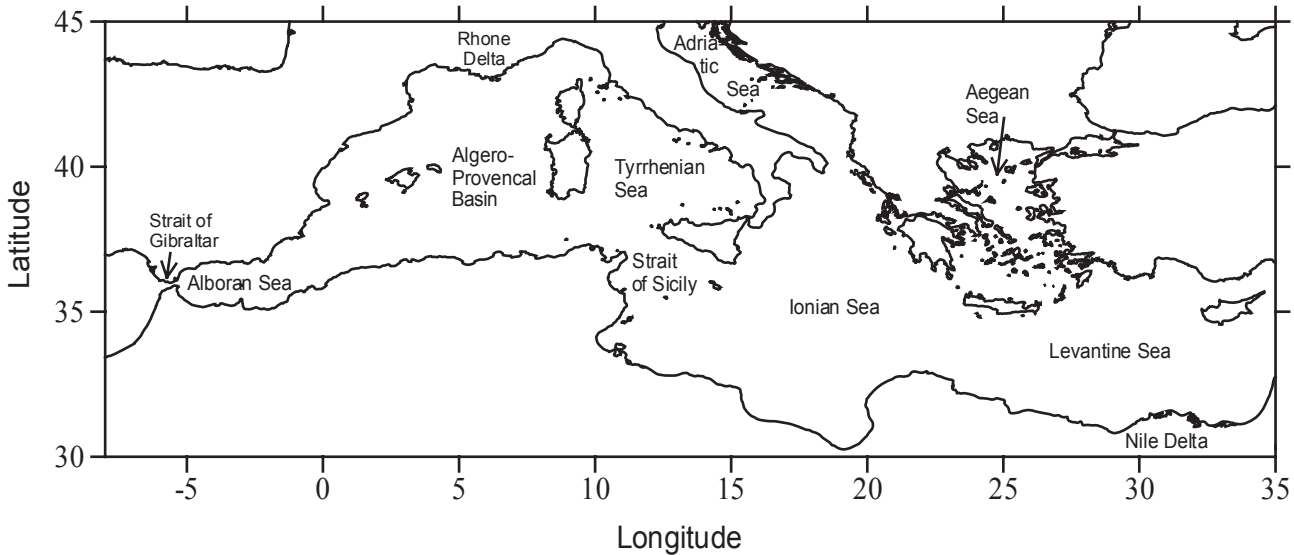


Figure 1.

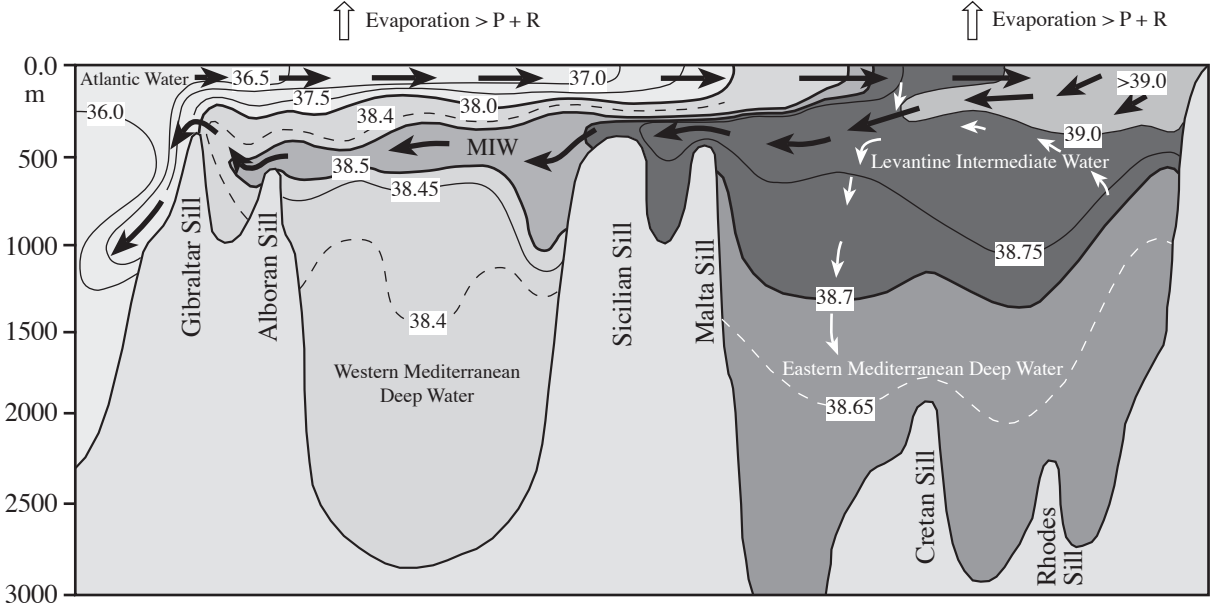


Figure 2.

EUROPE

45
N

40

35

30

AFRICA

0°

20°

40E

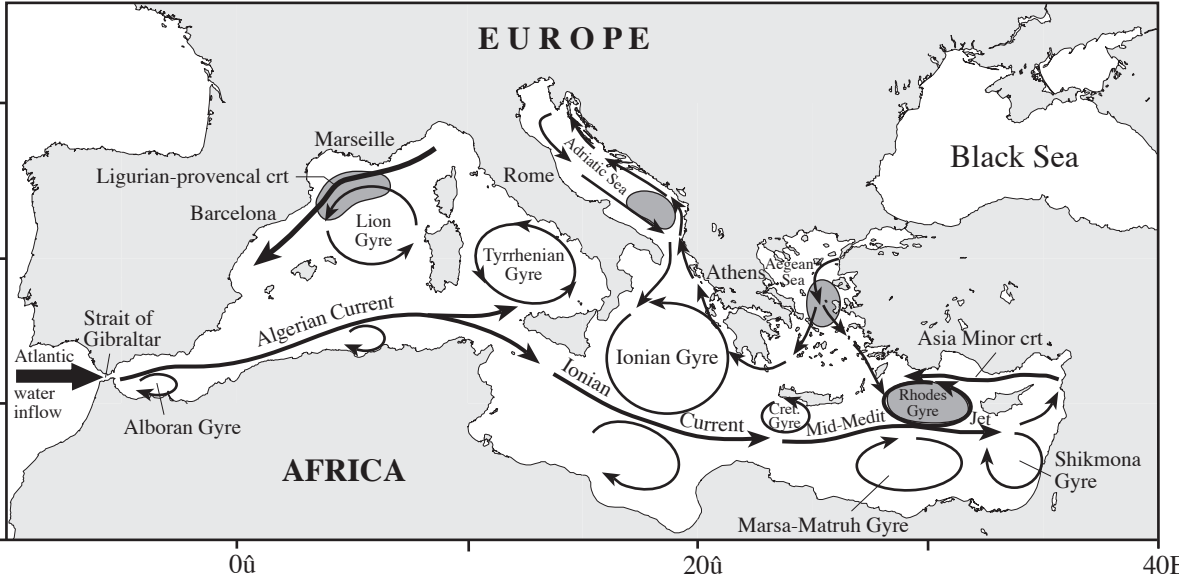


Figure 3.

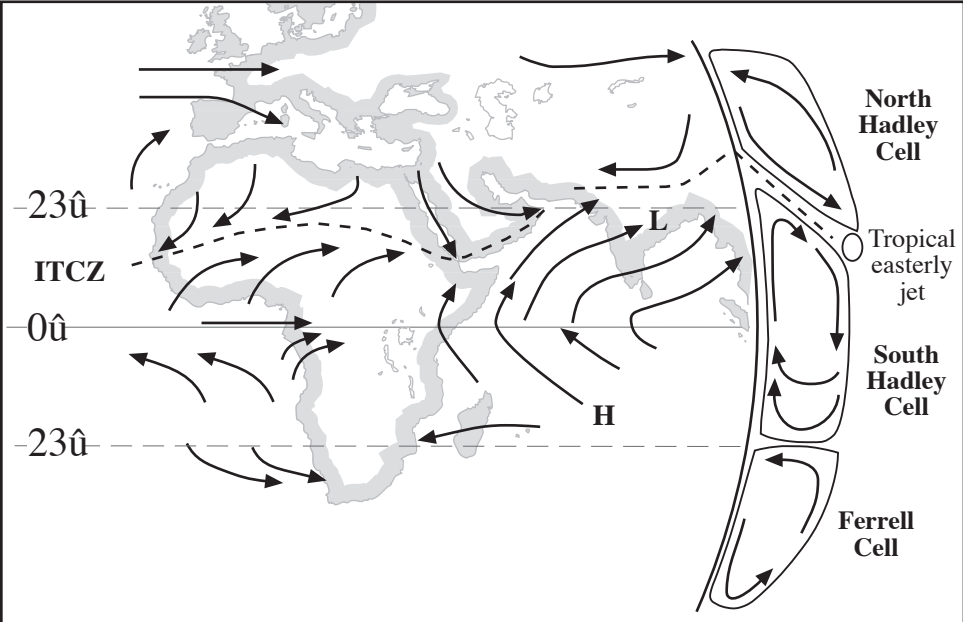


Figure 4.

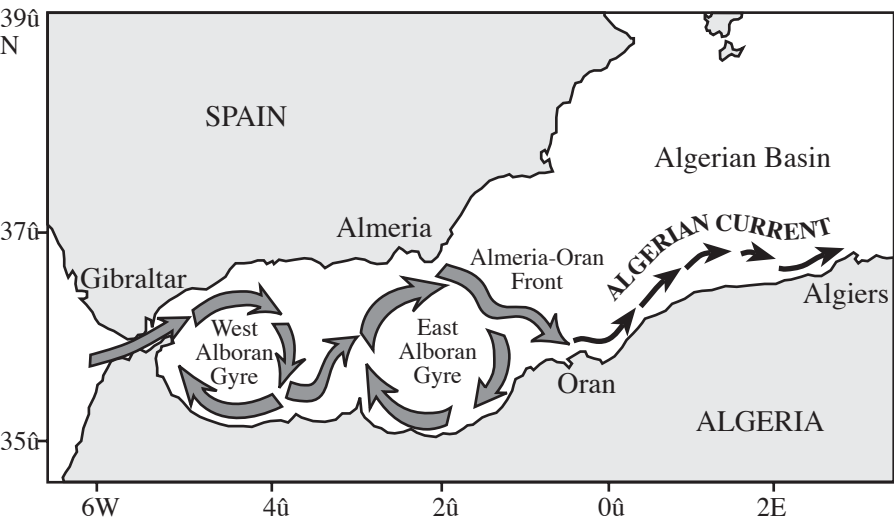


Figure 5.

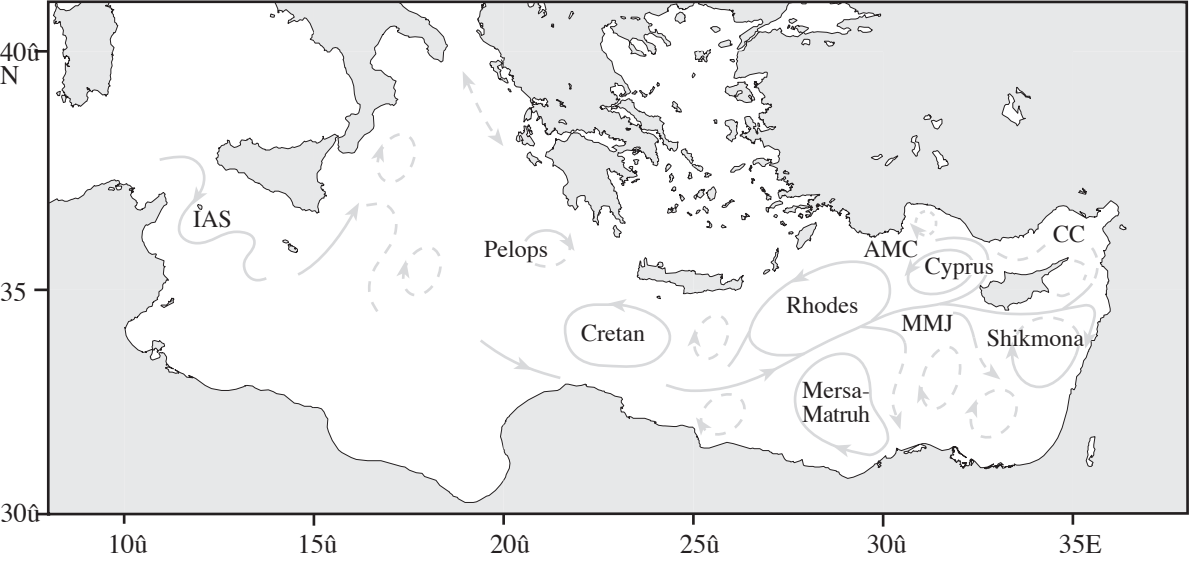


Figure 6.

Salinity (p.s.u.)

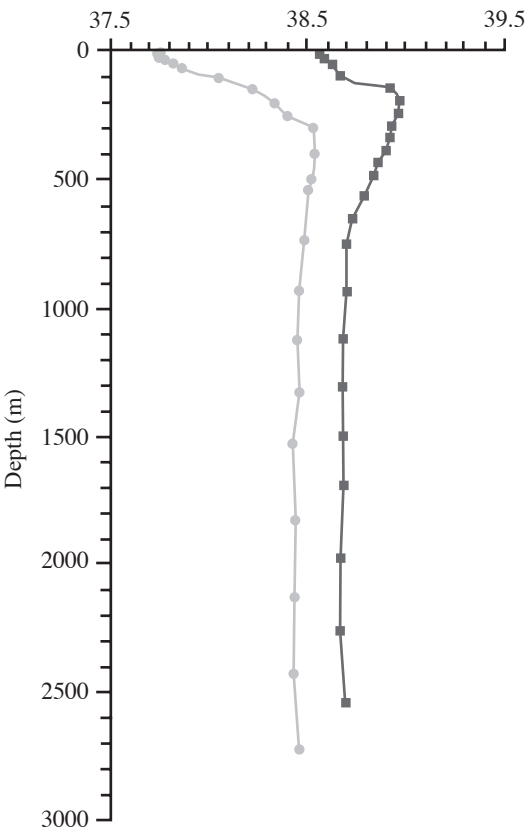
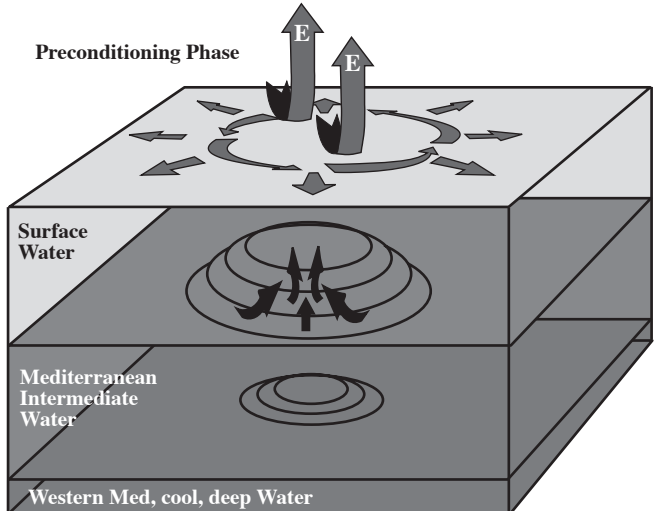


Figure 7.

Preconditioning Phase



Violent mixing and deep convection phases

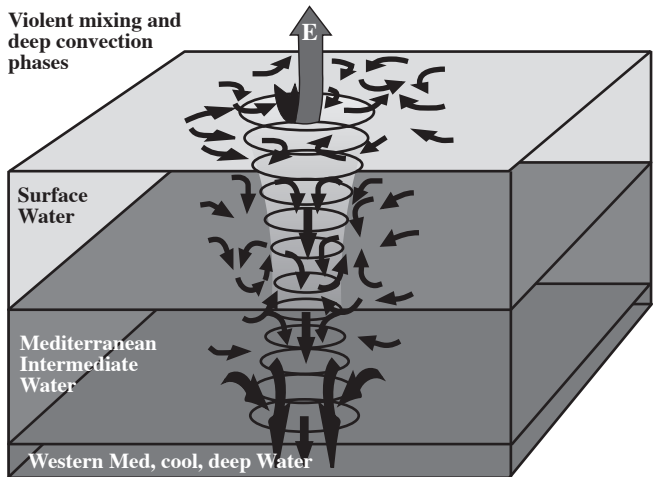


Figure 8.

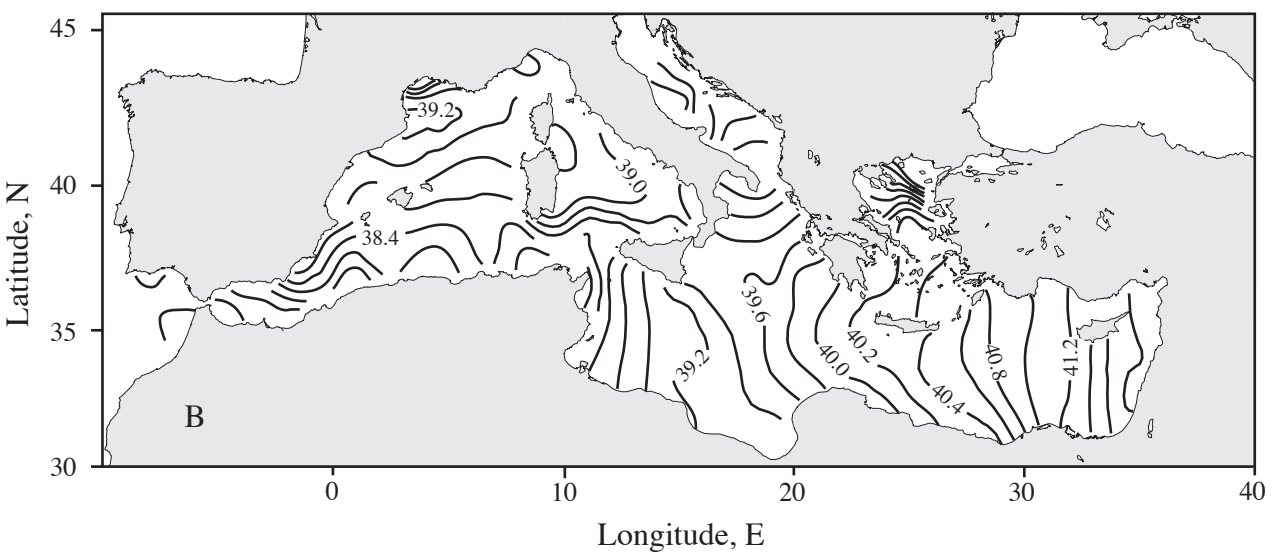
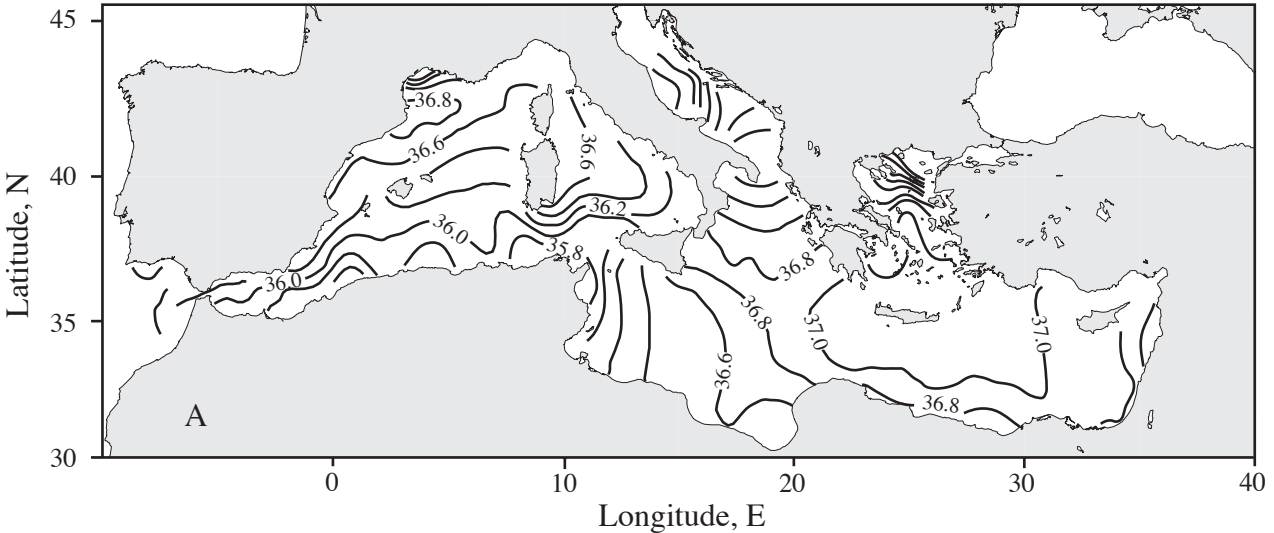
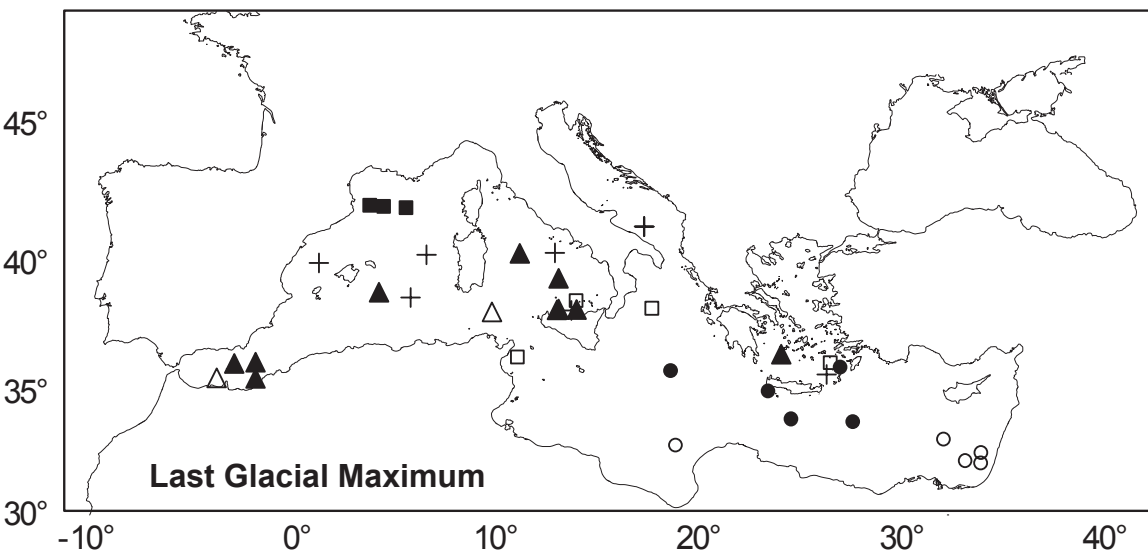
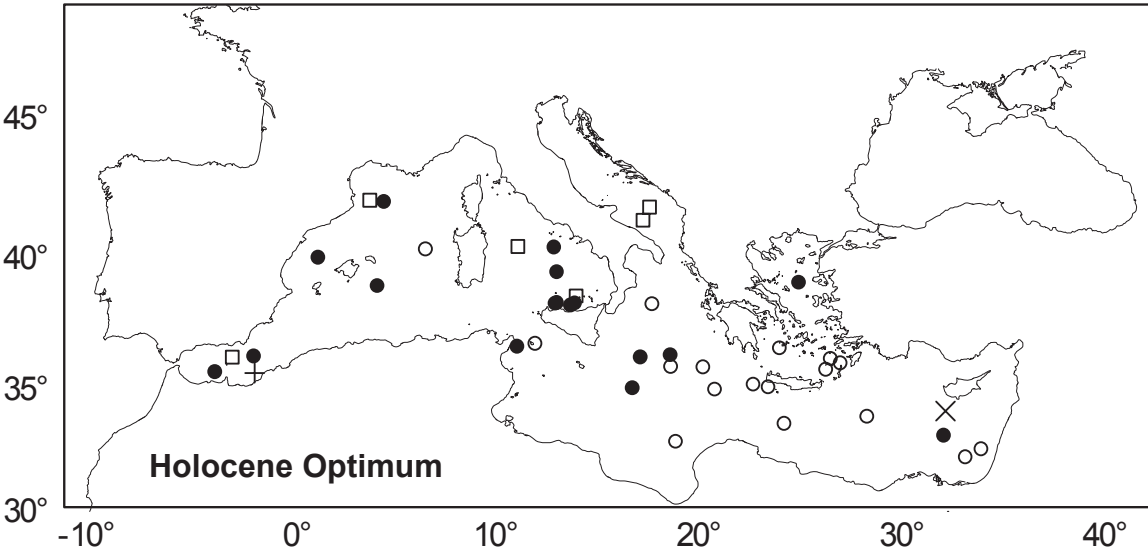
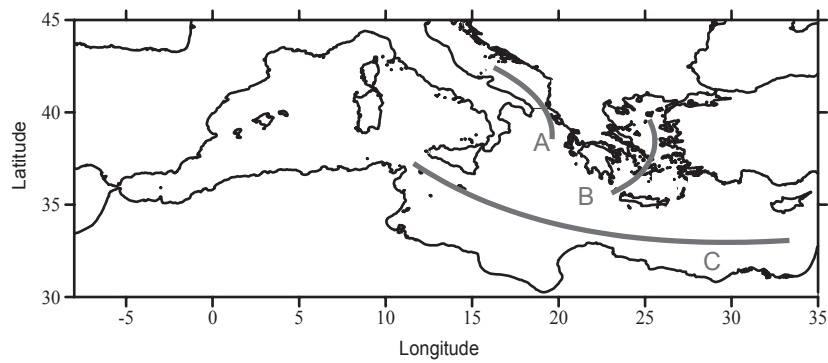


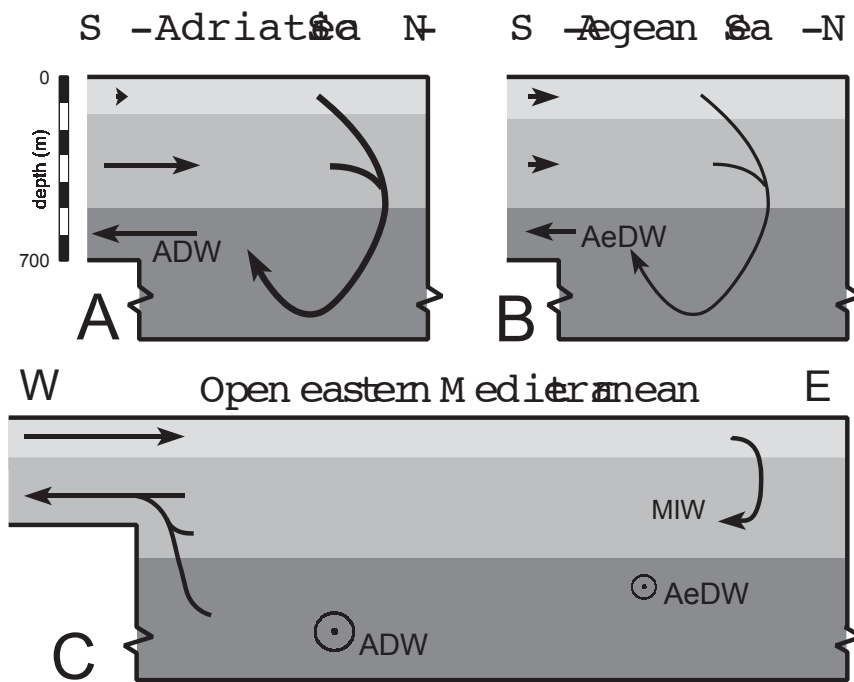
Figure 9.



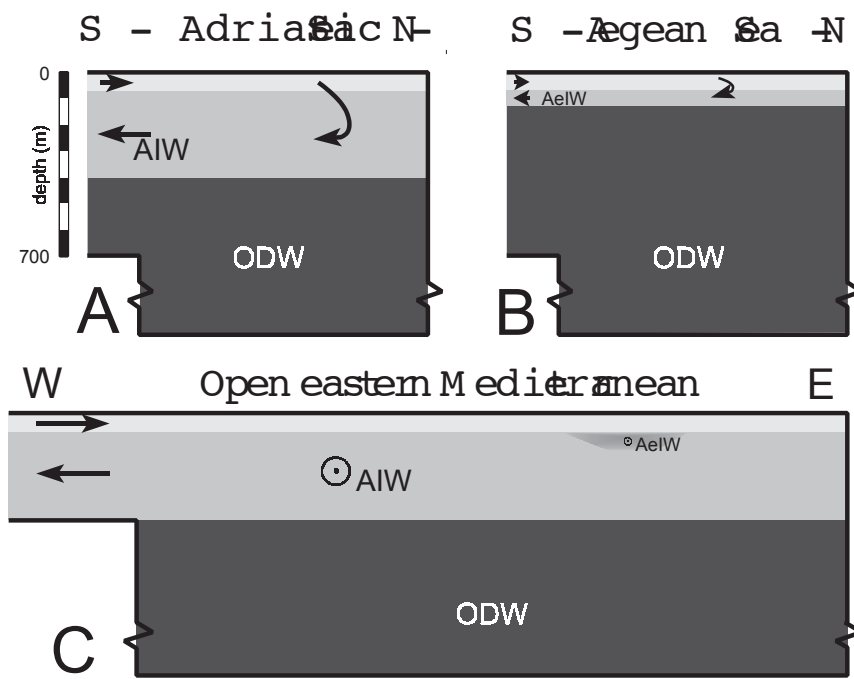
■ ▲ △ + □ ● ○ X
7+ 9+ 11+ 13+ 15+ 17+ 19+ 21+ C



Present-Day (pre 1988)

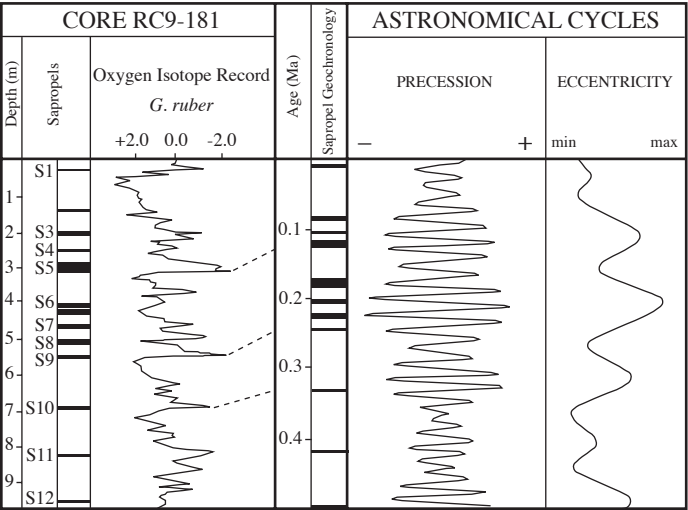


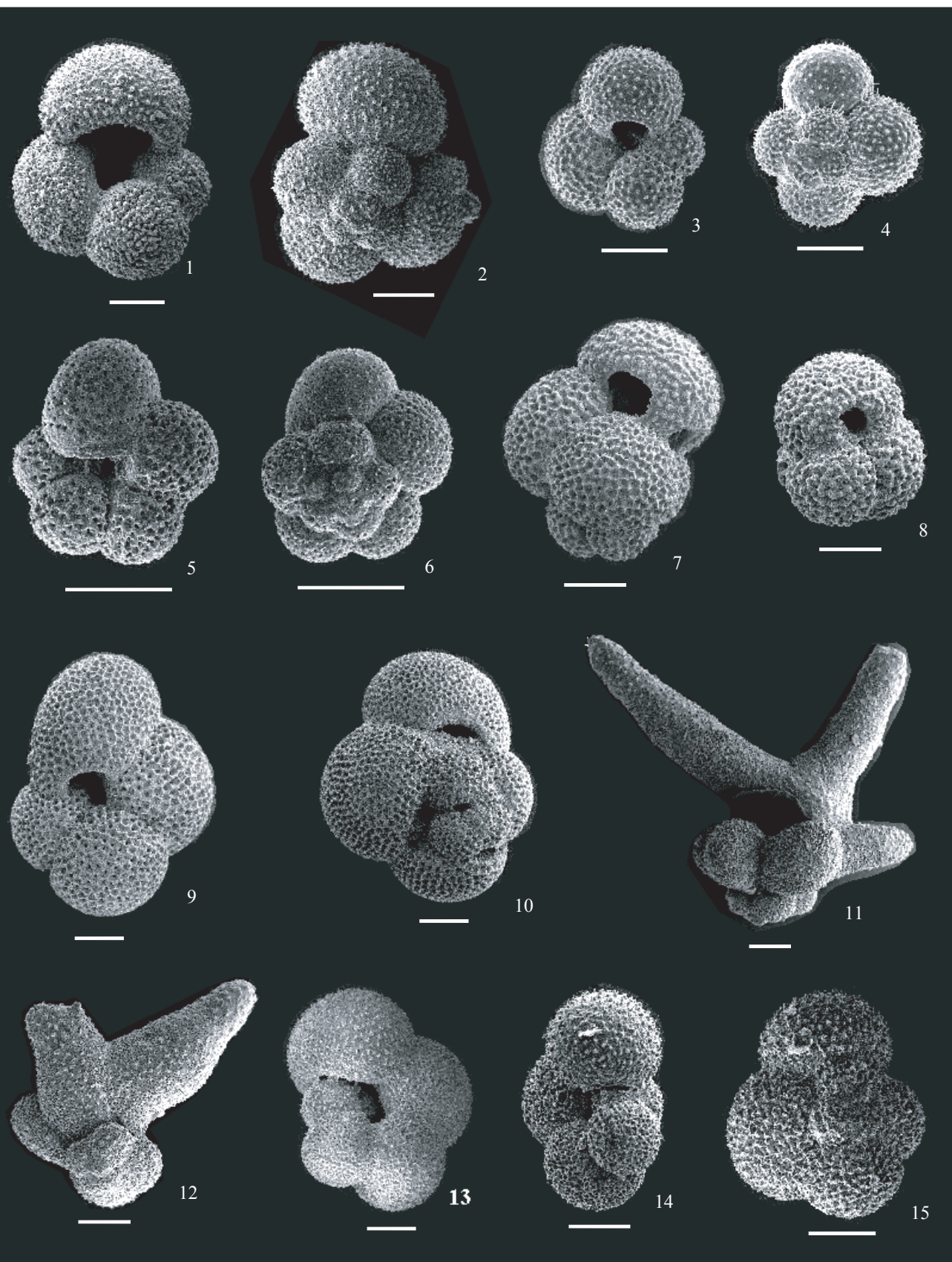
Sapropel-time



CORE RC9-181

ASTRONOMICAL CYCLES





TOP

SECT 6-4
SL 103
M51-3 #567

